Simulating dimethylsulphide seasonality with the Dynamic Green Ocean Model PlankTOM5

M. Vogt,[1] S. M. Vallina,[1] E. T. Buitenhuis,[1] L. Bopp,[2] and C. Le Quéré[1,3]

[1]   We study the dynamics of dimethylsulphide (DMS) and dimethylsulphoniopropionate (DMSP) using the global ocean biogeochemistry model PlankTOM5, which includes three phytoplankton and two zooplankton functional types (PFTs). We present a fully prognostic DMS module describing intracellular particulate DMSP (DMSPp) production, concentrations of dissolved DMSP (DMSPd), and DMS production and consumption. The model produces DMS fields that compare reasonably well with the observed annual mean DMS fields, zonal mean DMS concentrations, and its seasonal cycle. Modeled ecosystem composition and modeled total chlorophyll influenced mean DMS concentrations and DMS seasonality at mid- and high latitudes, but did not control the seasonal cycle in the tropics. The introduction of a direct, irradiation-dependent DMS production term (exudation) in the model improved the match between modeled and observed DMS seasonality, but deteriorated simulated zonal mean concentrations. In PlankTOM5, exudation was found to be most important for DMS seasonality in the tropics, and a variable DMSP cell quota as a function of light and nutrient stress was more important than a PFT-specific minimal DMSPp cell quota. The results suggest that DMS seasonality in the low latitudes is mostly driven by light. The agreement between model and data for DMS, DMSPp, and DMSPd is reasonable at the Bermuda Atlantic Time Series Station, where the summer paradox is observed.

Citation: Vogt, M., S. M. Vallina, E. T. Buitenhuis, L. Bopp, and C. Le Quéré (2010), Simulating dimethylsulphide seasonality with the Dynamic Green Ocean Model PlankTOM5, *J. Geophys. Res.*, *115*, C06021, doi:10.1029/2009JC005529.

1.   Introduction

[2]   Dimethylsulphide (DMS) is a climate relevant gas produced in marine ecosystems and emitted to the atmosphere [e.g., *Stefels et al.*, 2007], where it is oxidized to sulphate aerosol and involved in the formation of cloud condensation nuclei [*Charlson et al.*, 1987]. *Charlson et al.* [1987] suggested a potential feedback mechanism by which algae could impact climate through the regulation of the sulphur cycle. The so-called "CLAW hypothesis" states that algae may be able to influence CCN number density through DMS emissions as a response to increased temperatures and/or increased UV radiation. If this hypothesis were true, algae may be able to produce a negative feedback to global warming.

[3]   Despite the importance of DMS for the global sulphur cycle, the metabolical role of DMS in marine organisms is poorly known [e.g., *Stefels et al.*, 2007]. In marine ecosystems DMS is produced from its phytoplanktonic precursor particulate dimethylsulphoniopropionate (DMSPp).

The dimethylsulphoniopropionate (DMSP)-DMS system has been suggested to play a role in the osmoprotection of the cell [*Vairavamurthy et al.*, 1985; *Dickson and Kirst*, 1986, 1987a, 1987b], as a cryoprotectant [*Karsten et al.*, 1992, 1996], as an antioxidant [*Sunda et al.*, 2002] or as a grazing deterrent system [*Wolfe and Steinke*, 1996]. DMSPp is released to the water column upon cell lysis, during grazing [*Wolfe and Steinke*, 1996], through algal mortality [*Nguyen et al.*, 1988] or upon viral infection [*Malin et al.*, 1998]. Dissolved DMSP (DMSPd) can serve as a substrate for bacterial growth (reviewed by *Kiene and Slezak* [2006], and can be cleaved by several bacterial enzymes to DMS [*Todd et al.*, 2007, 2009; *Curson et al.*, 2008]. DMS itself can also be used as bacterial substrate for a set of specialist bacteria [*Vila-Costa et al.*, 2006], can be photolysed in the upper meters of the water column [*Brimblecombe and Shooter*, 1986; *Kieber et al.*, 1996] and is ventilated across the sea-air interface [*Liss and Slater*, 1974; *Zemmelink et al.*, 2004a, 2004b].

[4]   Several attempts have been made to simulate global DMS concentration patterns using diagnostic models [*Simó and Dachs*, 2002; *Belviso et al.*, 2004; *Vallina and Simó*, 2007]. Models using mixed layer depth and solar radiation dose as a proxy for DMS surface concentrations have been particularly successful in simulating observed surface concentration patterns and seasonality [*Simó and Dachs*, 2002; *Vallina et al.*, 2007]. A strong linear relationship between

[1]School of Environmental Sciences, University of East Anglia, Norwich, UK.
[2]Laboratoire des Sciences du Climat et de l'Environnement, IPSL, CEA Saclay, CNRS, Gif-sur-Yvette, France.
[3]British Antarctic Survey, Cambridge, UK.

observed DMS and solar radiation dose (SRD) in the mixed layer depth has been identified [*Vallina and Simó*, 2007], that accounts for more than 80% of the seasonal variability in the Sargasso Sea.

[5] The construction of global mechanistic models may shed light on the underlying mechanisms of DMS production in complex marine food webs. Current global prognostic DMS models are based on state-of-the-art multiplankton functional type models (Dynamic Green Ocean Models (DGOMs) [*Le Quéré et al.*, 2005]), and represent the DMS cycle with up to 3 sulphurous tracers (DMS, DMSPp and/or DMSPd) [*Bopp et al.*, 2008; *Six and Maier-Reimer*, 2006; *Chu et al.*, 2003]. Most prognostic models represent surface DMS patterns reasonably well in the mid- and high latitudes, where DMS and chlorophyll are tightly coupled, but some are unable to simulate the observed decoupling of DMS and chlorophyll-a in the low latitudes [e.g., *Six and Maier-Reimer*, 2006]: Between ca. 40°N and 40°S, DMS concentrations are maximal during the summer, when chlorophyll concentrations are at their lowest [*Vallina et al.*, 2006]. In contrast, DMS concentrations are low during the spring bloom, when chlorophyll values are maximal in this area. This behavior was called the "summer paradox" [*Simó and Pedrós-Alió*, 1999; *Toole et al.*, 2003]. A mathematical analysis of the system of equations describing the evolution of DMS in one prognostic model revealed that DMS dynamics were "slaved" to the dynamics of the ecosystem model [*Cropp et al.*, 2004]. Given that the model equations analysed by *Cropp et al.* [2004] are fairly similar to other equations used in current DMS model, this finding is likely to be representative for the characteristics of other DMS models. The authors conclude that decoupling between DMS and chlorophyll is difficult to achieve without an external forcing, a finding exploited, e.g., by *Lefèvre et al.* [2002]. Consequently, some authors opt for the inclusion of DMS source and sink terms with an explicit dependence on environmental conditions such as light, in order to achieve the observed decoupling [*Vallina et al.*, 2008].

[6] The Bermuda Atlantic Time Series Station (BATS) in the Sargasso Sea is one location where DMS measurements are available and which features the summer paradox [*Dacey et al.*, 1998]. Several 1-D prognostic DMS models have been tuned and applied to this location, but modelers still have to reach a consensus on which mechanism(s) are essential to explain the summer paradox. Species shifts, increased exudation due to light stress [*Sunda et al.*, 2002] and bacterial inhibition of DMS degradation [*Slezak et al.*, 2001] have been suggested as possible mechanisms to decouple DMS and chlorophyll, but 1-D DMS models reach decoupling using different mechanisms [*Lefèvre et al.*, 2002; *Toole et al.*, 2008; *Vallina et al.*, 2008].

[7] Here we present a new global fully prognostic DMS model that achieves decoupling of DMS and chlorophyll-a in parts of the low latitudes. In the first part of this paper we evaluate the results of our DMS model using DMS observations from *Kettle and Andreae* [2000]. We conduct a sensitivity analysis and discuss the main parameters influencing DMS concentration patterns. In the second part of our study, we focus on DMS seasonality and the summer paradox. We study the relative importance of ecosystem composition, species succession and the direct effect of light stress for the seasonal cycle of DMS. We show that direct release of DMS from phytoplankton is one possible mechanism through which the observed seasonality in the low latitudes can be simulated. We compare modeled and observed DMS(P) patterns at BATS and demonstrate that with a global model developed to represent global DMS seasonality it is possible to achieve a reasonable representation of DMS and DMSP at this site.

2. Model Description

2.1. Physical Sea-Ice-Ocean Coupled Model and Forcing

[8] We use the OPA8.1 ocean general circulation model (OGCM). OPA is a fully prognostic OGCM based on the primitive equations [*Madec et al.*, 1998]. The model output is projected onto the irregular ORCA grid, which has a longitudinal resolution of 2 degrees and a latitudinal resolution of 1.5° enhanced to 0.5° at the equator and at the poles. The vertical resolution is 10 m in the upper 100 m and comprises of 31 depth levels down to the ocean floor. The vertical eddy diffusivity and viscosity coefficients are calculated using a 1.5 order turbulent closure scheme which explicitly calculates mixed layer depth as a function of shear stress [*Gasper et al.*, 1990] and produces a minimum of diffusion in the thermocline. The sea-ice component of ORCA-LIM is the prognostic sea-ice model Louvain-La-Neuve Sea Ice Model (LIM [*Fichefet and Maqueda*, 1999; *Timmermann et al.*, 2005]). OPA-ORCA-LIM is forced with daily data from the NCEP reanalysis for precipitation, wind stress and cloud cover [*Le Quéré et al.*, 2007]. The model calculates its own heat flux using a bulk formulation. We use a constant freshwater input from rivers [*da Cunha et al.*, 2007].

2.2. Biogeochemical Model: PlankTOM5

[9] We use the state-of-the-art ocean biogeochemistry model PlankTOM5, which represents ecosystem dynamics based on plankton functional types (PFTs) [*Le Quéré et al.*, 2005]. PlankTOM5 represents 3 phytoplankton functional types (pPFTs): silicifiers (diatoms) and calcifiers (coccolithophores) and mixed phytoplankton (nanophytoplankton) and 2 zooplankton functional types (zPFTs): micro- and mesozooplankton. The prognostic variables for the 3 pPFTs are their total biomass in carbon units, iron, chlorophyll and silicium content for the silicifiers. For the two size classes of zPFTs, only the biomass is modeled. All PFTs are assumed to have a constant C:N:P ratio. The ratios of Fe:C and Chl:C are variable and fully determined by the model. Si:C is calculated for diatoms only.

[10] PlankTOM5 comprises 29 biogeochemical tracers. It simulates the full cycles of phosphate, silicate, carbon, oxygen and contains a simplified iron cycle. The current model version includes limitation of phytoplanktonic growth by a macronutrient (phosphate, nitrate and ammonium), silicate and iron. Phosphate and nitrate uptake are not independent. The phosphate/nitrogen pool undergoes nitrogen fixation and denitrification. The model also describes 8 further dissolved and particulate abiotic compartments: dissolved inorganic carbon (DIC), dissolved oxygen and alkalinity, semilabile dissolved organic matter (DOM), small (organic) and big (ballasted) sinking particles, $CaCO_3$ and SiO_2. The model includes a ballast effect based on Stoke's Law [*Buitenhuis et al.*, 2001], and calculates the sinking

Table 1. Parameters for the DMS Module of PlankTOM5

Parameter	Label	Value	Reference
DMSPp cell quota			
Diatoms	q_{lit}^{dia} (q^{dia})	0.002 (0.0008–00046)	*Stefels et al.* [2007]
Nanophytoplankton	q_{lit}^{nano} (q^{nano})	0.01 (0.004–0.23)	*Stefels et al.* [2007]
Coccolithophores	q_{lit}^{cocco} (q^{cocco})	0.012 (0.0048–0.0276)	*Stefels et al.* [2007]
Ratio of DMS/DMSP released in grazing	α_{dms}	0.1	*Archer et al.* [2002]
Fraction of DMSPp released as DMSPd			
Microzooplankton grazing	λ_{Pi}^{mic}	0.74	*Buitenhuis et al.* [2006]
Mesozooplankton grazing	λ_{Pi}^{mes}	0.59	*Buitenhuis et al.* [2006]
DMS exudation rates			
Diatoms	λ_{dia}^{exud}	0.005 d^{-1}	
Nanophytoplankton	λ_{nano}^{exud}	0.05 d^{-1}	
Coccolithophores	λ_{cocco}^{exud}	0.05 d^{-1}	
Fraction of DMSPd cleaved by free DMSP lyase	λ^{DL}	0.01 d^{-1}	*Archer et al.* [2002]
Bacterial T dependence (Q_{10} = 3)	D	1.116	E. Buitenhuis (personal communication, 2007)
Microbial yield for bacterial DMSPd-DMS conversion	λ^{bac}	0.1	*Zubkov et al.* [2001]
Bacterial half saturation constants			
For DMSPd	K_{DMSP}^{bac}	1.08×10^{-9} mol DMS m^{-3}	*Archer et al.* [2002]
For DMS	K_{DMS}^{bac}	1.25×10^{-9} mol DMSP m^{-3}	*Archer et al.* [2002]
Photolysis rate	λ^{light}	0.05 d^{-1}	L. Bopp (personal communication, 2006)
Maximal PAR	PAR_{max}	80 W m^{-2}	this model

speed of big particles from the concentration of carbonate (CaCO$_3$) and silicate (SiO$_2$).

[11] The evolution of each prognostic variable T in the model is governed by the processes of advection, diffusion and biogeochemical transformation, as described in equation (1)

$$\frac{dT}{dt} = \nabla(\vec{u}T) + \nabla(\vec{K}\nabla T) + SMS. \quad (1)$$

The first right-hand term of equation (1) stands for advection, with $\vec{u}$ being the 3-D velocity vector of advection. The second term stands for diffusion, with $\vec{K}$ representing the 3-D tracer diffusion coefficients. Biogeochemical processes are expressed as the balance between biological source and sink terms (SMS; Sources Minus Sinks). The air-sea fluxes of trace gases are parameterized according to *Wanninkhof* [1992] and are included in the SMS terms.

[12] The biogeochemical model is initialized with observations of DIC and alkalinity from the Global Ocean Data Analysis Project (GLODAP [*Key et al.*, 2004]) and with nutrient fields for phosphate, silicate and oxygen from the World Ocean Atlas (2001). The biogeochemistry is forced with dust input of iron and silicate [*Tegen and Fung*, 1995]. The biological variables in the model are initialized using simulated tracer concentrations from a previous model run.

2.3. DMS Module of PlankTOM5

[13] We added three additional variables describing the DMS cycle in PlankTOM5: The model simulates dimethylsulphide (DMS), particulate dimethylsulphoniopropionate (DMSPp) and dissolved DMSP (DMSPd) concentrations and their cycling within the marine food web. All equations are semiempirical and take into account current experimental constraints on the parameters used. Within the observational range of parameter uncertainty, the model has been tuned to optimize the representation of DMS seasonality. Equations describing the dynamics of PFT biomass have been adopted from PlankTOM5 without modifications.

The sulphur mass budget is not closed and sulphur is never limiting to DMSP synthesis by the 3 pPFTs. However, sulphur cycling is constantly limited by the flow rates between ecosystem constituents. A list of all parameters used in the DMS module of PlankTOM5 is given in the Table 1 of this paper for the standard run.

2.3.1. Dynamics of DMSPp, DMSPd, and DMS

[14] The dynamics of DMS, DMSPp and DMSPd (concentrations in $\frac{mol}{L}$) are described according to the following time-dependent equations:

$$DMSPp = \sum_{i=i}^{3} q_i * P_i, \quad (2)$$

$$\frac{\partial DMSPd}{\partial t} = \sum_{i=1}^{3} \left[\left((1 - \alpha_{dms}) * \left(\lambda_{Pi}^{mic} * g_{Pi}^{mic} + \lambda_{Pi}^{mes} * g_{Pi}^{mes} \right) + m_{Pi} \right) * q_i \right]$$
$$- \lambda^{DL} * DMSPd - \phi_{DMSP}^{bac} * DMSPd, \quad (3)$$

$$\frac{\partial DMS}{\partial t} = \sum_{i=1}^{3} \left[\left(\alpha_{dms} * \left(\lambda_{Pi}^{mic} * g_{Pi}^{mic} + \lambda_{Pi}^{mes} * g_{Pi}^{mes} \right) + m_{Pi} \right. \right.$$
$$\left. + \lambda^{exud_i} * \frac{PAR}{PAR_{max}} * P_i \right) * q_i \right] + \lambda^{bac} * \phi_{DMSP}^{bac} * DMSPd$$
$$+ \lambda^{DL} * DMSPd - \lambda^{light} * PAR * DMS$$
$$- \phi_{DMS}^{bac} * DMS - F^{DMS}, \quad (4)$$

where q_i is the internal cell quota for DMSP for the 3 different pPFTs P_i, i = 1, 2, 3 and t is time. P_i are the pPFT carbon concentrations ($\frac{mol(C)}{L}$). α_{dms} describes the ratio of DMS/DMSP release after cell lysis. g_{Pi}^{Z} describes the amount of P_i grazed by zPFT Z. m_{Pi} is the mortality of pPFT P_i for each time step. The parameters λ_{Pi}^{Z} are the fractions of DMSPp grazed by zPFT Z_i that are available for further processing within the water column. λ^{DL}, λ^{exud}, and λ^{light} are constant scaling parameters for grazing, cleavage by free DMSP lyase, exudation, and photolysis. λ^{bac} is a scaling constant for the bacterial efficiency of DMSP to DMS conversion. The functions ϕ describe bacterial degradation rates.

The indices *mic* and *mes* indicate micro- and mesozooplankton contributions to DMS and DMSP release in grazing $\left(\frac{mol(C)}{Lt}\right)$, *bac* describes terms related to bacteria. F^{DMS} is the sea-to-air flux of DMS [*Wanninkhof*, 1992; *Saltzman et al.*, 1993].

2.3.2. DMSPp Cell Quota

[15] The DMSPp cell quota of a PFT q_i describes the ratio of sulphur to carbon for each pPFT P_i. In laboratory and field experiments, this quota has been observed to vary with algal taxon, species, and environmental conditions (temperature, nutrient status, solar radiation dose; reviewed, e.g., by *Stefels et al.* [2007]). Given the large observed differences in DMSPp quota between different species of the same algal taxon and the large range of DMSPp levels observed within one species as a function of environmental stress, the cell quota of the 3 pPFTs are only poorly constrained. Here, we use a literature value, q_{lit}, suggested by *Stefels et al.* [2007] as a benchmark for the 3 modeled pPFTs. The simulated cell quota is allowed to vary as a function of both light (PAR) and nutrient (Fe, PO_4) stress [*Sunda et al.*, 2002] (s_1, s_2, s_3) and is temperature (T) dependent. The T dependence simulates the function of DMS and DMSP in cryoprotection [*Karsten et al.*, 1992, 1996]. It has been set to enhance the quota for temperatures of 0°C or below. Hence, the DMSP cell quota for pPFT P_i is described as

$$q_i = (\max(s_1, s_2, s_3, 0.3)*2. - f_{corr})*\left(1 + \frac{1}{(T + 2.5)^6}\right)*q_{lit}, \quad (5)$$

where

$$s_1 = \frac{PAR}{PAR_{max}}, \quad (6)$$

$$s_2 = \frac{K_{Fe}^i}{Fe + K_{Fe}^i}, \quad (7)$$

$$s_3 = 0.7*\frac{K_{PO_4}^i}{PO_4 + K_{PO_4}^i}, \quad (8)$$

with the K_N^i being the phytoplanktonic half saturation constants for nutrient N and each PFT P_i, and f_{corr} an adjustable correction factor to tune global DMSPp concentrations, currently set to 0.25. Taking into account all the above terms, q_i can vary between 0.4 and ca. 2.3 × q_{lit}, which is consistent with observational variations in cell quota [*Stefels et al.*, 2007]. Due to their definition, the environmental stressors s_1, s_2 and s_3 are dominant at different latitudes: While light stress is dominant at tropical and subtropical latitudes, PO_4^- stress is greatest in temperate waters and Fe stress is maximal in the Southern Ocean (not shown). Hence, light stress is expected to be most important for the simulation of the summer paradox.

2.3.3. Grazing, Mortality, and Biomasses

[16] Grazing of microzooplankton on any given pPFT is described by the following equations in PlankTOM5 [*Buitenhuis et al.*, 2006]:

$$g_{P_i}^{mic} = G_{max}^{mic}*a^T*\frac{p_{P_i}^{mic}*P_i}{K_{P_i}^{mic} + \sum_j p_{F_j}^{mic}*F_j}*MIC, \quad (9)$$

and similarly for mesozooplankton

$$g_{P_i}^{mes} = G_{max}^{mes}*b^T*\frac{p_{P_i}^{mes}*P_i}{K_{P_i}^{mes} + \sum_j p_{F_j}^{mes}*F_j}*MES, \quad (10)$$

where $g_{P_i}^Z$ is the amount of pPFT P_i that is grazed by zPFT Z_j per timestep. G_{max}^Z is the maximal grazing rate for zPFT Z_j at 0°, a and b are the temperature (T) dependences of grazing, and $p_{F_i}^Z$ is the preference for food F_i. MIC and MES are the biomasses of micro- and mesozooplankton and $K^{Z,i}$ is the zooplanktonic half saturation constant for grazing. All other growth and loss terms, such as the phytoplanktonic mortality rates, and the biomasses for both pPFT and zPFT are also derived directly from PlankTOM5.

[17] In the DMSP module, the ratio of DMSPd/DMS produced in grazing is described according to equations (3) and (4). α_{DMS} describes the ratio of DMS to DMSPd released in grazing processes. It is assumed to be 1:9 [*Archer et al.*, 2002]. The constants λ_{Pi}^Z have been defined in agreement with those for the cycling of carbon within the zooplankton grazers [*Buitenhuis et al.*, 2006]. This means that the fate of ingested DMSPp (loss through sloppy feeding or respiration, incorporation into biomass, excretion) is coupled to the fate of ingested carbon.

[18] All in all, a total 74% of DMSPp ingested by microzooplankton and a total of 59% ingested by mesozooplankton is released to the liquid phase as DMSPd and is available for further biological processing [*Buitenhuis et al.*, 2006]. (Fraction of grazed carbon incorporated into the body mass of the grazers: 26%, fraction of carbon released to the water column due to 'sloppy feeding': 11%, fraction respired: 33%, fraction excreted into the seawater: 30%. Hence, a total of 74% of ingested carbon is released. We assume that 50% of DMSPp excreted by mesozooplankton is exported (M. Steinke, personal communication, 2006). Thus, only 59% of DMSPd ingested by mesozooplankton is available for further processing.)

2.3.4. Exudation/Leakage

[19] Based on the findings reported by *Vallina et al.* [2008] a term leading directly from phytoplankton to DMS as a function of environmental conditions has been implemented in the model. We call this term the "exudation term," despite the current lack of experimental evidence for such direct transfer of DMS across the cell membrane. The direct release of DMS from phytoplanktonic cells is in agreement with *Sunda et al.* [2002], i.e., DMS may be part of an oxidant chain triggered under light and nutrient stress.

[20] The modeled exudation of DMS is assumed to be light dependent and proportional to the intracellular DMSPp concentration. Given that there are no experimental constraints on DMS exudation rates, we assumed the lowest possible exudation rates that still allowed decoupling in the tropics and were consistent with observed DMS concentrations. Thus, the so-derived exudation rates are a factor 4 lower than those used by *Vallina et al.* [2008] and vary with phytoplankton group. Exudation of DMS by diatoms was set to be 10× lower than the exudation rates of the other pPFTs, in analogy to the ratio used by *Archer et al.* [2002] for DMSP exudation. The exudation of DMSPd by phyto-

plankton has been neglected. Thus, the exudation term is parameterized as

$$\left(\frac{\partial DMS}{\partial t}\right)_{exudation} = \lambda^{exud} * \frac{PAR}{PAR_{max}} * DMSPp, \quad (11)$$

with λ^{exud} being a constant rate term (see Table 1) and PAR the light available for photosynthesis.

2.3.5. Cleavage of DMSP by Free DMSP Lyase

[21] In seawater, a small fraction of DMSPd is cleaved by free DMSP lyase [*Scarratt et al.*, 2000]. The suspended DMSP lyase is assumed to originate from DMSP lyase containing algae and to be released after cell lysis. The cleavage by DMSP lyase is parameterized as a small and constant proportion (λ^{DL}, Table 1) of the DMSPd concentration

$$\left(\frac{\partial DMSP}{\partial t}\right)_{cleavage} = -\lambda^{DL} * DMSPd. \quad (12)$$

2.3.6. Bacterial Degradation of DMSPd

[22] PlankTOM5 parameterizes bacterial remineralization of organic matter, but does not include an explicit formulation for bacterial biomass. We use an implicit formulation following *Aumont and Bopp* [2006], where bacterial biomass is a function of zooplankton biomass, multiplied by a depth profile (see below). Bacterial degradation is then parameterized using normalized biomass and a bacterial activity on DMSPd. Thus,

$$\phi^{bac}_{DMSPd} = \mu^{bac}_{max} * L^{bac}_{tot} * d^T * B, \quad (13)$$

where μ^{bac}_{max} is the maximal bacterial growth rate (0.6 d^{-1}), L^{bac}_{tot} the total nutrient limitation for bacteria, d^T the temperature dependence of growth and B the dimensionless normalized bacterial biomass. The bacterial temperature dependence d^T has been chosen, so that $Q^{bac}_{10} = 3$, i.e., $d = 1.116$. The individual terms are calculated as

$$L^{bac}_{tot} = \min\left(L^{bac}_{nut}, \frac{DMSPd}{DMSPd + K^{bac}_{DMSPd}}\right) * L^{bac}_{light}, \quad (14)$$

$$L^{bac}_{nut} = \min\left(\frac{PO_4}{PO_4 + K^{bac}_{PO_4}}, \frac{Fe}{Fe + K^{bac}_{Fe}}, \frac{DOC}{DOC + K^{bac}_{DOC}}\right), \quad (15)$$

$$L^{bac}_{light} = \min\left(1., \max\left(0.66, 1. - \left(\frac{PAR}{PAR_{max}}\right)^6 + 0.18\right)\right), \quad (16)$$

$$B = \frac{0.7*(MIC + 2*MES)}{B_{norm}} * \min\left(1, \frac{depth_c}{depth}\right), \quad (17)$$

with L^{bac}_{nut} being the bacterial nutrient limitation of the model, excluding DMSPd, L^{bac}_{light} being the bacterial limitation of DMSPd degradation as a function of insolation [*Slezak et al.*, 2001]. Bacterial activity is a function of the nutrient availability of both DOM and DMSP and parametrized using the minimum of 4 Michaelis-Menten functions, with PO_4 phosphate, Fe iron and DOC dissolved organic matter concentrations. The K^{bac}_N are the bacterial half saturation

constants for the respective nutrient N, with $122*K^{bac}_{PO4} = 0.1$ μmol L^{-1}, $K^{bac}_{Fe} = 0.025$ nmol L^{-1} and $K^{bac}_{DOC} = 5$ μmol L^{-1}. Bacterial biomass is calculated implicitly using a regression with zooplankton biomass and depth ($depth_c = 120$ m), and normalized to a standard value ($B_{norm} = 4*10$ μmol C L^{-1}). This relationship was obtained from a correlation of output from a version of the PISCES model containing an explicit representation of bacteria (O. Aumont, personal communication, 2006).

2.3.7. Bacterial Degradation of DMS

[23] The formulation for bacterial degradation of DMS closely resembles the one used to simulate bacterial degradation of DMSPd. However, different half saturation constants were used for DMS and DMSPd [*Archer et al.*, 2002]. Hence,

$$\phi^{bac}_{DMS} = \mu^{bac}_{max} * L^{bac}_{tot} * d^T * \alpha^{bac} * B, \quad (18)$$

with B and d^T as above and

$$L^{bac}_{tot} = \min\left(L^{bac}_{nut}, \frac{DMS}{DMS + K^{bac}_{DMS}}\right) * L^{bac}_{light}. \quad (19)$$

[24] Based on *Vila-Costa et al.* [2006], we assume that approximately 33% (α^{bac}) of the bacterial community can utilize DMS. In the model, DMS degrading bacteria are limited both by the availability of DOC and of DMS, which is expressed by calculating the minimum of 4 Michaelis-Menten functions as above.

2.3.8. Photolysis of DMS

[25] At present, PlankTOM5 does not simulate the propagation of UV light through the water column. Hence, despite the fact that DMS photolysis is driven mainly by UV wavelengths, the photolysis rate for DMS is assumed to be a linear function of incident PAR and DMS concentration. PAR and UV are approximately linearly related in surface waters on cloud free days and on a monthly average [see, e.g., *Vantrepotte and Mélin*, 2006, Figure 2.1, p. 25]. Furthermore, DMS is not directly photolysed in seawater [*Brimblecombe and Shooter*, 1986; *Brugger et al.*, 1998], but oxidized by free radicals created through the photolysis of coloured dissolved organic matter (CDOM). CDOM concentrations, however, are not modeled in PlankTOM5, and hence our equations are a function of light (PAR) only. The rate constants used are within the experimental range of uncertainty for the Sargasso Sea [*Bailey et al.*, 2008; *Toole and Siegel*, 2004]

$$\left(\frac{\partial DMS}{\partial t}\right)_{photolysis} = -\lambda^{light} * PAR * DMS, \quad (20)$$

where λ^{light} is given in Table 1.

2.3.9. Sea-Air Fluxes of DMS

[26] The sea to air flux of DMS is given by the product of sea-to-air transfer velocity and the difference in concentration of DMS across the sea-air interface [*Liss and Slater*, 1974]. Because the air concentration is assumed to be negligible, the general flux equation is simplified to

$$F_{air} = k_w * DMS_{aq}, \quad (21)$$

where DMS_{aq} is the sea surface concentration of DMS. The sea to air fluxes are calculated according to *Wanninkhof*

Table 2. Settings for the Four Runs in PlankTOM5 Used for the Study of the Influence of Ecosystem Composition on DMS Patterns

Name of Run	Stress Cell Quota	Exudation	PFT Specific Cell Quota
PlankTOM5-SEP	yes	yes	yes
PlankTOM5-SNEP	yes	no	yes
PlankTOM5-SENP	yes	yes	no
PlankTOM5-NSENP	no	yes	no

[1992] as a square function of wind speed and temperature. The Schmidt number for DMS has been calculated according to *Saltzman et al.* [1993].

3. Model Setup

3.1. General Description

[27] We run PlankTOM5 including the sulphur cycle starting from 1992 to 2007. DMSP and DMS have been initialized with concentrations of zero nM everywhere, and the module has been run until it reached steady state. An equilibrium between DMS(P) source and sink terms was reached after 7 years of calculation (no more major changes in DMS concentrations). The equilibrium time scale has been found empirically and corresponds to the equilibrium time of the biogeochemistry model [*da Cunha et al.*, 2007], i.e., the timescale beyond which total annual mean tracer concentrations remain constant for constant forcing. We use the simulation of year 2006 for all output fields. The interannual variability of global mean surface DMS concentrations is low during 1999–2007 (global annual mean surface DMS varies by less than 0.1%), so that the use of one arbitrary year during this time period is representative.

3.2. Studying the Controls on DMS Seasonality

[28] We use 4 sensitivity experiments in order to investigate the impact of light and ecosystem composition on DMS concentration patterns, the seasonality of DMS and the coupling between DMS and chlorophyll-a (Table 2): Run 1 (referred to as "SEP," i.e., "Stress-Exudation-PFT") is the standard run, as described above. This run includes the direct DMS exudation term from phytoplankton and a PFT-specific DMSPp cell quota varying with light and nutrient stress. Run 2 ("SNEP," i.e., "Stress-No Exudation-PFT") includes a PFT-specific and stress-dependent DMSPp cell

quota, but does not include the exudation term. This run was tuned to best fit the observed annual concentration means and DMS seasonality in the tropics. PlankTOM5-SNEP was constructed to demonstrate how much decoupling of DMS and chlorophyll is possible when parameters are kept within the range of observational constraints and when external forcings do not influence DMS patterns directly. All parameters are as for the standard run, but minimal DMSPp cell quota had to be doubled in order to get realistic DMS fields. The doubling of all cell quota did not affect DMS seasonality, but adjusted overall DMSPp levels to be within the observed range. Run 3 ("SENP") has a variable but PFT-independent cell quota and includes exudation. Run 4 ("NSENP") has a constant DMSPp cell quota for all PFTs and includes exudation. These runs are used to test the effect of ecosystem composition on DMS concentration patterns and DMS seasonality and to study the coupling between DMS and chlorophyll-a.

4. Results

4.1. Model Evaluation: Chlorophyll-a and Ecosystem Composition

[29] Table 3 summarizes the diagnostics used to evaluate PlankTOM5 in OPA. The model results for primary production (57.4 Pg C yr^{-1}) fall within the range of estimates based on observational data [*Behrenfeld and Falkowski*, 1997]. Model export production (9.1 Pg C yr^{-1}) is only slightly below observational estimates (11 Tg C yr^{-1} [*Schlitzer*, 2004]). While microzooplankton grazing is close to observational estimates [*Calbet*, 2001], mesozooplankton grazing on phytoplankton is overestimated by the model [*Calbet and Landry*, 2004], although the uncertainty in the data is large. Based on marker pigment measurements [*Uitz et al.*, 2006], *Le Quéré et al.* [2005] estimated the biomasses of all 3 pPFTs to be around 0.1–0.4 Pg C yr^{-1}. PlankTOM5 may slightly overestimate total phytoplanktonic biomass, but given the large uncertainty in the association of pigment data with biomass, this estimate can only serve as a coarse indicator of the relative abundance of these groups (Table 3). Modeled and observed chlorophyll-a are compared in Figure 1. The agreement between model and data is reasonable, especially in the Southern Ocean. However, PlankTOM5 underestimates chlorophyll concentrations in the Arctic, in the North Atlantic and in most of the upwelling regions.

Table 3. Model Evaluation in PlankTOM5

Variable	Observation (Pg C yr^{-1})	PlankTOM5 (Pg C yr^{-1})	Reference for Observational Value
Primary Production	50–70	57.4	*Behrenfeld and Falkowski* [1997]
Export at 100 m	10–12	9.1	*Schlitzer* [2004]
Microzooplankton grazing[a]	29	28.2	*Calbet* [2001]
Mesozooplankton grazing[a]	5.5	18.5	*Calbet and Landry* [2004]
Biomasses of PFTs[b]			
Diatoms (micro-)	0.11	0.63	*Le Quéré et al.* [2005]
Mixed phytoplankton (pico- + $\frac{2}{3}$ nano-)	0.54	0.48	*Le Quéré et al.* [2005]
Coccolithophores ($\frac{1}{3}$ nano-)	0.13	0.34	*Le Quéré et al.* [2005]
Total phytoplankton	0.78	1.46	*Le Quéré et al.* [2005]
Total DMS flux (Tg S yr^{-1})	15–33	24.0	*Kettle and Andreae* [2000]

[a]Grazing on phytoplankton only.
[b]PFT equivalent of observational groups calculated as indicated in parentheses.

(a) Chlorophyll-a from SeaWifs (mg m^{-3})   (b) Chlorophyll-a from PlankTOM5 (mg m^{-3})
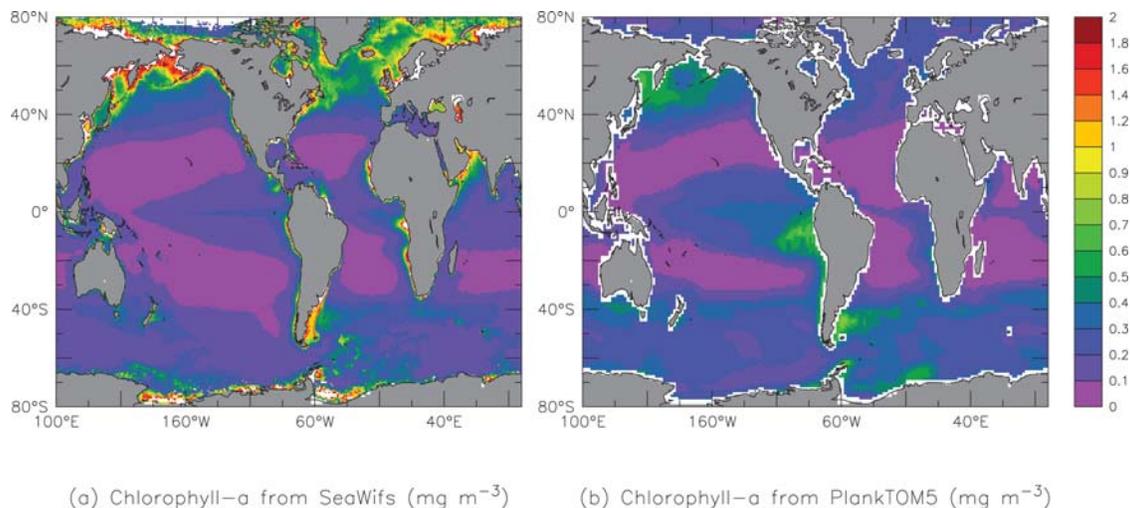
Figure 1. Comparison of annual mean chlorophyll-a for (a) SeaWiFS satellite observational data and (b) PlankTOM5.

[30] Figure 2 shows the relative dominance of the 3 pPFTs and their nearest corresponding satellite-derived group from PHYSAT [*Alvain et al.*, 2005]. For the sake of simplicity, we use the satellite-derived group of diatoms for the silicifiers, coccolithophores for the calcifiers and nanoeukaryotes for nanophytoplankton. In the observations, regions in white correspond to regions where none of the 3 PFT discussed above is dominant. In the model results, white areas are either characterized by the lack of one group that constitutes more than 50% of total chlorophyll or by chlorophyll concentrations less than 0.3 mg m^{-3}. This threshold was set because the low chlorophyll regions are observed to be dominated by Prochlorococcus and Synechococcus-like picophytoplankton [*Alvain et al.*, 2008], groups that are not represented in PlankTOM5. As a consequence, the low latitudes are modeled to be dominated by coccolithophores and mixed phytoplankton. A dominance value of 1 means that the PFT is dominant in 12/12 months, whereas a value of 0 means that it is not dominant in any of the months.

[31] Figures 2a and 2b show the relative dominance of diatoms in both model and data. PlankTOM5 underestimates diatom dominance in the northern parts of the Southern Ocean, but represents dominance patterns well close to the Antarctic continent. The model slightly overestimates diatom dominance in the Arctic and in the North Atlantic and North West Pacific. The annual relative nanophytoplankton dominance is in good agreement with the dominance of its satellite-derived analogue for the Southern Ocean (Figures 2c and 2d). In the Northern Hemisphere (NH), nanophytoplankton dominance is consistently underestimated by the model. Furthermore, PlankTOM5 predicts a nanophytoplankton dominance in the Equatorial Pacific, which is not present in the observations. For the coccolithophores (Figures 2e and 2f), the agreement between modeled and satellite-derived populations is reasonable in the NH. The model predicts slightly higher dominance of coccolithophores in the Arctic. As discussed by *Alvain et al.* [2006], this group is likely to be underestimated by the satellite measurements, so that higher Arctic dominance values are possible.

[32] Figure 3 shows the observed and simulated biomass of the two zooplankton functional types, microzooplankton (Figures 3a and 3b) and mesozooplankton (Figures 3c and 3d). A throrough validation of the two zooplankton functional types been performed by *Buitenhuis et al.* [2006] and E. Buitenhuis et al. (Biogeochemical fluxes through microzooplankton, submitted to *Global Biogeochemical Cycles*, 2009). While the distributions of mesozooplankton from modeled and observed estimates match well, the microzooplankton biomass is underestimated. In particular, the model cannot reproduce high concentrations of microzooplankton on the continental shelves and in coastal areas. This may partly be due to large seasonal fluctuations in microzooplankton biomass, which are not captured by the model. In addition, there is uncertainty in the carbon conversion factors used to convert zooplankton counts into biomass, which may lead to overestimates of the observations. However, distributions in the Southern Ocean as well as in parts of the Atlantic (40°N–40°S) seemed to be captured well by the model.

4.2. Model Results: DMS, DMSPp, and DMSPd (Standard Run)

4.2.1. Global Annual Mean Surface Concentrations

[33] The first and second columns in Table 4 contain the main statistical characteristics for the globally integrated average DMS surface concentrations compared to DMS from *Kettle and Andreae* [2000]. PlankTOM5 simulates an integrated global annual surface mean of 1.9 nM, which is similar to the estimates by *Kettle and Andreae* [2000] (1.6 nM). However, PlankTOM5 underestimates maximal DMS concentrations. This is mostly because high coastal DMS values cannot be simulated in the model. The analysis of the 95 percentile as a proxy for open ocean concentrations show a better agreement between model (95% of concentrations below 5.77 nM) and data (95% of data below 5.43 nM). PlankTOM5 underestimates the global spread of DMS concentrations, as given by the standard deviation. The calculation of the cost function to quantify model-data agreement according to *Allen et al.* [2007] gives the value of
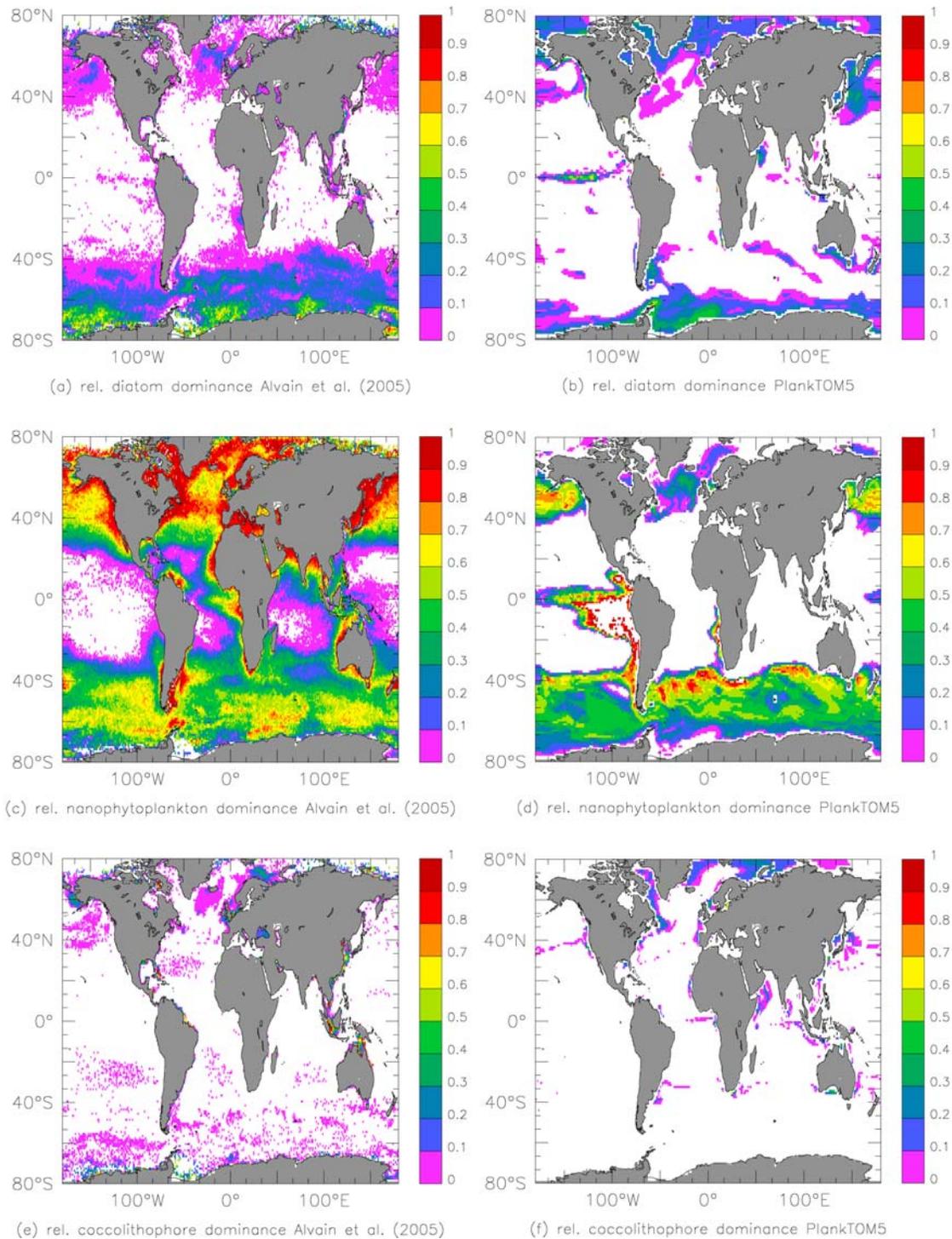
Figure 2. Comparison of the relative dominance of the three pPFTs with estimates from satellite observations using (a) PHYSAT data [*Alvain et al.*, 2005, 2006], (b) diatoms, (c and d) nanophytoplankton, and (e and f) coccolithophores.

cf = 0.94 for the standard run, with cf<1 belonging to the category of "very good agreement" [*Maréchal*, 2004].

[34] We now compare annual mean DMS concentrations on the basin scale. The simulated annual average surface concentrations of DMS (Figure 4b) compare reasonably well with the interpolated climatology of Figure 4a [*Kettle and Andreae*, 2000]. Annual mean DMSPp and DMSPd

concentrations are shown in Figures 4c and 4d. While the model is able to simulate some of the high DMS concentrations in the Arctic, it underpredicts DMS concentrations in the polar waters of the Southern Ocean. This is most likely due to an underprediction of DMSPp in this region (Figure 4c), which is potentially due to the absence of an explicitly modeled group of the haptophyte *Phaeocystis*, a
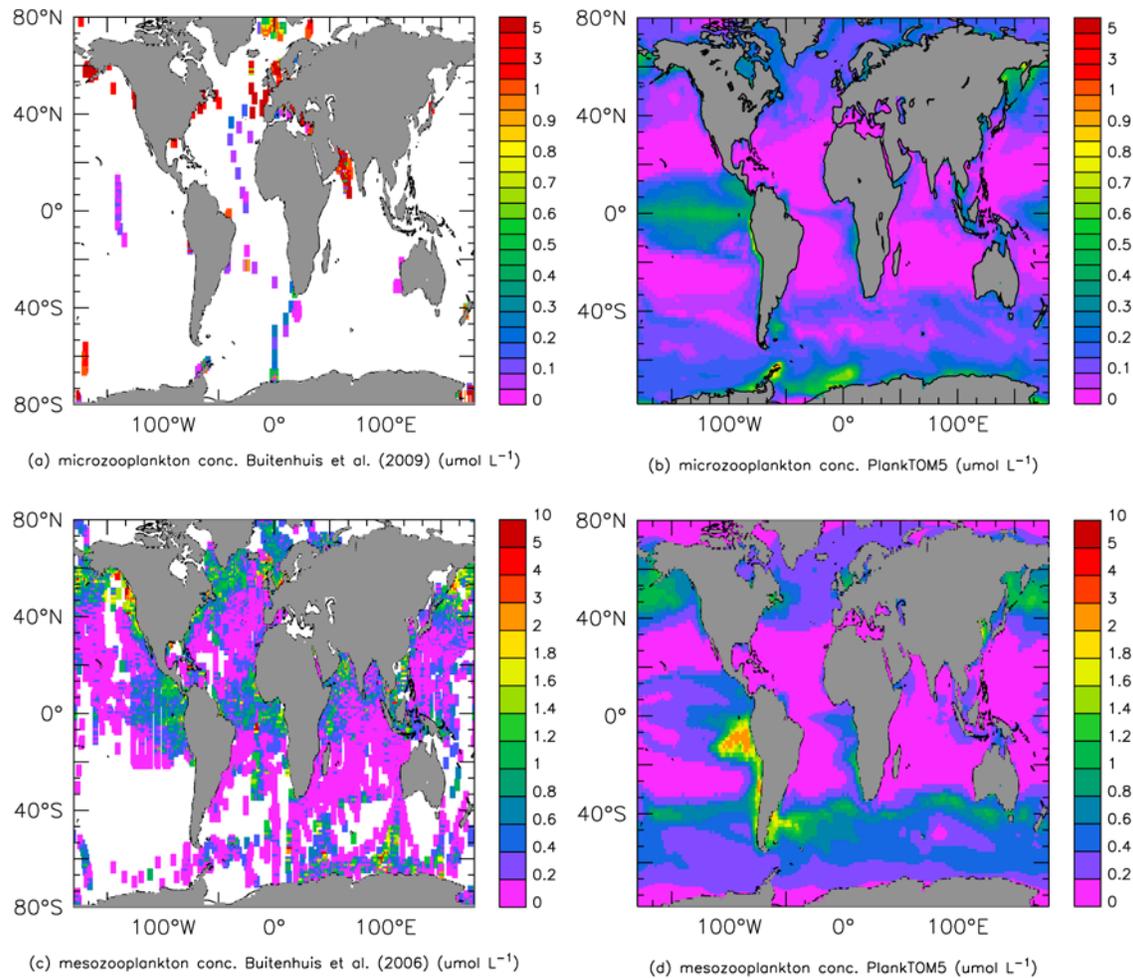
Figure 3. Comparison of observed and modeled biomass of the two zPFTs, (a and b) micro- and (c and d) mesozooplankton. Microzooplankton and mesozooplankton biomass in μmol L^{-1}.

group known to be prolific DMS producers and to be abundant in the Southern Ocean. The modeled Southern Ocean plankton community is dominated by diatoms, which are poor DMS producers [*Keller et al.*, 1989]. Simulated DMS concentrations are in good agreement with the data in the Indian Ocean, but PlankTOM5 underestimates DMS concentrations in the Equatorial Pacific and the Northern North Atlantic. There is no comprehensive global database for DMSPd and DMSPp concentrations, so a global comparison of model and data is difficult. Both DMSPp and DMSPd, however, are within the range measured in the North Atlantic during the AMT programme [*Bell et al.*, 2006], and modeled and observed DMSP concentrations are in agreement for the BATS Station (see analysis in section 4.3.3).

4.2.2. Zonal Mean DMS and Chlorophyll

[35] We compare zonal mean distributions of DMS and chlorophyll from observations [*Kettle and Andreae*, 2000] with our model results (Figure 5). Zonal variations in DMS are larger in the interpolated data (black line) than in the model. In particular, modeled zonal means for the standard run (PlankTOM5-SEP) are almost constant in the low latitudes (Figure 5 (top), PlankTOM5-SNEP see section 4.3). A Spearman rank correlation between observed zonal mean

DMS (Figure 5 (bottom)) and observed zonal mean chlorophyll (smoothed using a Hanning filter [*Blackman and Tukey*, 1959]) gives a correlation coefficient of $\rho = 0.26$, which is low due to the high variability in chlorophyll. However, the amplitudes of observed zonal mean chlorophyll and DMS covary: Local maxima and minima in DMS and chlorophyll coincide spatially (e.g., around 70°S, 40°S

Table 4. Statistical Assessment of Global Annual Mean Surface DMS Concentrations[a]

Statistical Quantity	Kettle and Andreae [2000] (nM)	PlankTOM5 (SEP) (nM)	SNEP (nM)	SENP (nM)	NSENP (nM)
Global maximum DMS	26.57	5.92	15.15	5.65	6.91
Global minimum DMS	0.00	0.54	0.52	0.45	0.41
Global spread	1.93	0.76	2.34	0.78	1.01
Global mean	1.56	1.90	2.54	1.66	1.79
95% of data below	5.43	5.77	6.41	5.53	5.66
CF[b]	–	0.94	0.79	1.05	1.03

[a]Model results for the four test runs, and comparison to observational data.

[b]Model-data agreement for 95 percentile of DMS concentrations $CF = \frac{1}{n}\sum \frac{|D-M|}{\sigma_D}$, where D is the observational data, M is the model data, and σ_D is the standard deviation observations [*Allen et al.*, 2007; *Maréchal*, 2004].
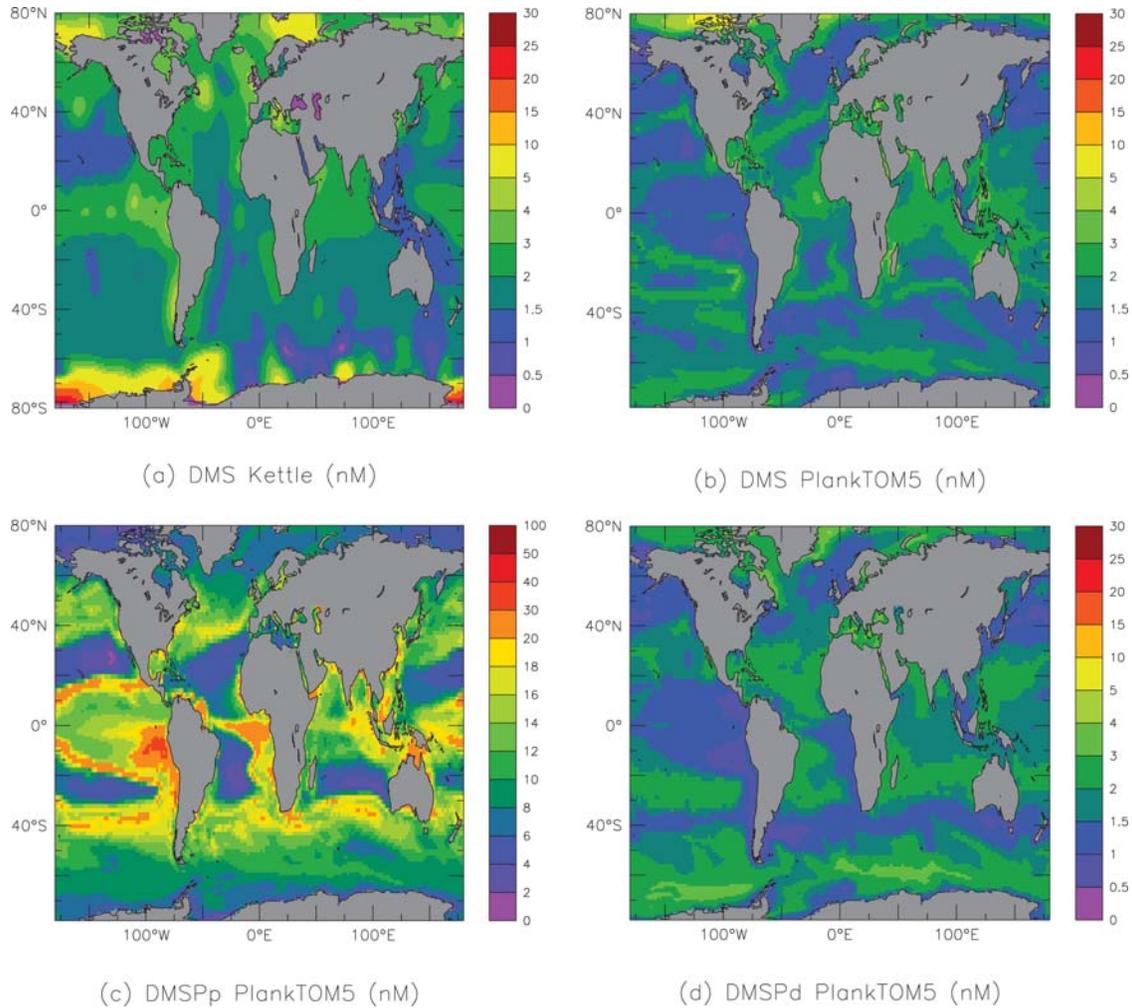
Figure 4. Annual mean DMS surface concentration fields in nmol L^{-1} (nM) for (a) DMS from *Kettle and Andreae* [2000], (b) simulated DMS, (c) simulated DMSPp, and (d) simulated DMSPd from the standard run of PlankTOM5 (PlankTOM5-SEP).

and 0° (maxima) and between 50–60°S, as well as around 25 °S and 25°N (minima)) for latitudes between 70°S and 60°N. Modeled chlorophyll (red line) is in good agreement with observed chlorophyll for 70°S–40°N, but the model underpredicts the chlorophyll concentrations in the NH, where coastal values strongly influence zonal mean chlorophyll. Despite the underprediction of chlorophyll between 40°N–60°N, simulated DMS concentrations are consistent with observations. The model cannot capture the differences in gradients between DMS and chlorophyll levels between 40°N–60°N, which is clearly visible in the observations.

[36] To compare model-data agreement in terms of absolute concentrations, we calculate the Spearman correlation coefficient between model and two DMS datasets for the 95 percentile (values less than 6 nM) of surface DMS (1) binned in zonal average band of 10° and (2) in 10° × 20° boxes (latitude × longitude). We use both the interpolated DMS data [*Kettle and Andreae*, 2000] and the Global Surface Sea (GSS) DMS Database (http://saga.pmel.noaa.gov/dms/), containing ca. 30,000 data points (1972–2003). The correlations for the zonal averages are reasonably good (ρ = 0.62 for DMS$_{PlankTOM}$ vs. DMS$_{Kettle}$ and ρ = 0.47 for

DMS$_{PlankTOM}$ vs. DMS$_{GSS}$), but they become considerably lower when the data is analysed using the 10° × 20° boxes (ρ = 0.34 for DMS$_{PlankTOM}$ vs. DMS$_{Kettle}$ and ρ = 0.28 for DMS$_{PlankTOM}$ vs. DMS$_{GSS}$, respectively). Hence, the model has some skill when large regions with similar environmental properties are considered, but much less skill when regional properties matter more strongly for the averages.

4.2.3. Parameter Sensitivity of the DMS Module

[37] We now analyse the sensitivity of the DMS module to its parameters. To (From) each parameter of the DMS module, 50% of its absolute value is added (subtracted). The model is then run for four years from the equilibrated state and the results are compared with those from the control run for the same year. We use the global annual surface mean DMS, DMSPd and DMSPp concentrations and study their deviations in % from the original value (DMS_c) upon perturbation (DMS_p) of one of the model parameters. The differences are calculated as the integrated means of $\Delta_{pn} = \frac{DMS_c - DMS_p}{DMS_c} * 100$, with p_n designating the nth parameter of the sulphur system (Table 1). For bacterial temperature dependence ($ba(T) = d^T$; see equation (13)), we add (subtract) 0.5 to (from) the assumed Q$_{10}$ value of 3, rather than multiplying
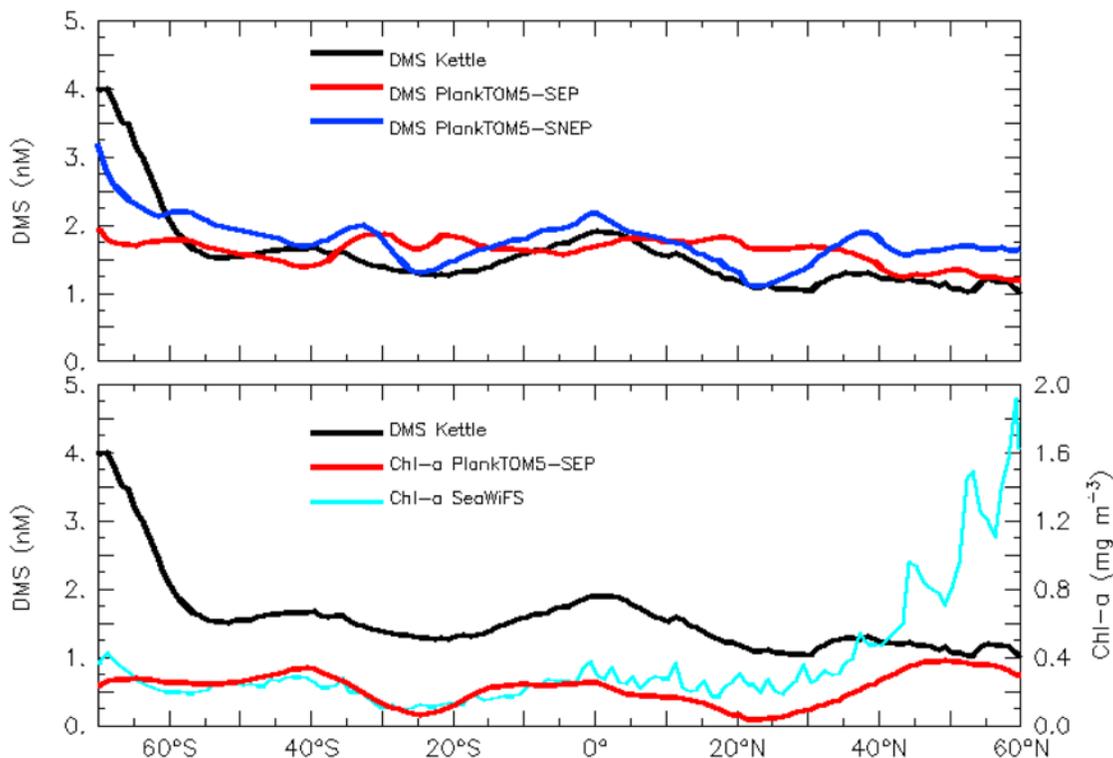
Figure 5. (top) Zonal mean DMS from *Kettle and Andreae* [2000] (black line), results from PlankTOM5-SEP (standard run, red line), and from PlankTOM5-SNEP (no exudation, blue line). (bottom) DMS from *Kettle and Andreae* [2000] (black line), chlorophyll-a from the SeaWiFS satellite (turquoise line), and from PlankTOM5 (red line). Zonal mean DMS concentrations covary with chlorophyll a for wide regions of the ocean, but not in the Northern Hemisphere.

the temperature dependence *d* directly by 1.5, because this parameters enters our equations to the power of *T*. Therefore, this strategy prevents biasing our sensitivity study towards an artificially inflated sensitivity to this parameter. We find that the response of the model is nearly symmetric with respect to positive and negative perturbations in parameter space. Thus, we only discuss the results from positive perturbations in the following.

[38] In the case of an increase of the parameters by 50%, DMS proves to be most sensitive to changes in the Q_{10} of bacterial activity (–74%), the cell quota of all 3 PFTs (+44%), and to changes of the exudation rate (+26%), as well as to changes of the individual, PFT specific cell quota (+0.9%, +18% and +25%) and exudation rates (+0.1%, +9% and +16%) for diatoms, nanophytoplankton and coccolithophores, respectively. DMSPd surface concentrations are most sensitive to changes in bacterial activity (–73%), a change of all cell quota (+44%) and of the individual cell quota (+1%, +18% and +24%) for diatoms, nanophytoplankton and coccolithophores, respectively. In addition, a change of the bacterial half saturation constant for DMSPd consumption leads to a change of +7% in the annual means. DMSPp is directly sensitive to changes in overall cell quota (+50%), and also to changes in the individual PFT-specific cell quota (+2%, +22% and +26% for silicifiers, mixed phytoplankton and calcifiers, respectively). Indirectly, DMSPp is sensitive to an increase of bacterial temperature dependence (+33%), which leads to a slightly faster

recycling of nutrients and hence slightly increased algal growth. In order to visualize the order of importance for the factors controlling their dynamics, we normalize DMS, DMSPp and DMSPd sensitivities to 100% (Figure 6), i.e.,

$$\Theta\Delta_{pi} = \frac{|\Delta_{pi}|}{\sum_{j=1:n}^{n} |\Delta_{pj}|}.$$

[39] The importance of the individual parameters is not constant but varies strongly with latitude (not shown). The importance of cell quota is linked to PFT distribution (more important for locations populated by mixed phytoplankton and coccolithophores containing large amounts of DMSP:C). Exudation rates and the bacterial temperature dependence have the highest impact on zonal mean DMS concentrations in the tropics. Bacterial temperature dependence is crucial for the balance between mean DMS concentration levels in the high and temperate latitudes and those in the low latitudes.

4.3. DMS Seasonality and the Summer Paradox

4.3.1. Seasonality of DMS, DMSPp, and DMSPd (Standard Run)

[40] Figure 7 shows the seasonal cycle of simulated DMS (Figure 7a), DMSPp (Figure 7c) and DMSPd (Figure 7d) and total chlorophyll (Figure 7e) in a Hovmøller diagram (time-latitude plot), with DMS and chlorophyll compared to observational data (Figures 7b and 7f; SeaWiFS [*Kettle and Andreae*, 2000]). The "boomerang shape" in DMS, DMSPd and DMSPp with 2 maxima in surface DMS concentrations

in the low latitudes and only one maximum in the high latitudes is a symptom of the summer paradox. While DMS and chlorophyll are both elevated during the summer months in the high latitudes, there is no such correlation in the low latitudes, where chlorophyll is almost constant.

Figure 6. Sensitivity of DMS-PlankTOM5 (SEP) to a perturbation in parameter space by +50% on global average (a) DMS (b) DMSPd, and (c) DMSPp. Parameters sensitivity was normalized to 100% ($\Theta_{\Delta P_T}$). Here ba(T) is bacterial temperature dependence d in d^T, scq is phytoplankton DMSP cell quota (all PFTs), exudr is exudation rate (all PFTs), fp is fraction of fecal pellets unavailable for further processing of DMSP content, grdms is fraction of DMS directly produced in grazing, dlc is DMSP lyase cleavage, photor is photolysis rate, km_{dmd} is bacterial half saturation constant DMSPd, km_{dms} is bacterial half saturation constant DMS, myield is microbial yield for DMSPd to DMS conversion.

[41] On basin scale, the seasonal correlation (quantified by a Spearman rank correlation coefficient) between model and data [*Kettle and Andreae*, 2000] is high in the North Atlantic ($\rho = 0.94$), the North ($\rho = 0.79$) and Subtropical Pacific ($\rho = 0.81$) and the Antarctic ($\rho = 0.94$) and Southern Ocean ($\rho = 0.69$). DMS seasonality in the Southern Ocean ($\rho = 0.69$) is reasonable, even though the model cannot reproduce the high amplitude of the seasonal cycle if DMS observed in the high latitudes. In general, correlations are lower in the equatorial regions than in the subtropical and high latitude oceans (Table 5). It is important to stress, however, that the uncertainty associated with the seasonal interpolation of the data is variable, as it critically depends on the wealth of data for each month and province [*Kettle et al.*, 1999].

4.3.2. Mechanisms Causing the Decoupling of DMS and Chlorophyll Between 40°N and 40°S (Summer Paradox)

[42] The parameter sensitivity tests performed in section 4.2.3 investigated the importance of the parameters of the DMS module for global annual mean DMS surface concentrations. In order to examine which processes control the global seasonality of DMS we show results from four separate runs, described in section 3.2 and listed in Table 2. In particular, we focus on DMS seasonality in the low latitudes, where the summer paradox [*Simó and Pedrós-Alió*, 1999; *Toole et al.*, 2003] has been observed. These tests not only include variations in parameter space, but involve modifications on the process level: Key processes which we identified to be most important for DMS seasonality were switched on and off. The results of the four models are summarized in Table 4, and annual mean fields are shown in Figure 8.

[43] The inclusion of a strong light dependence in PlankTOM5 (PlankTOM5-SEP), as suggested by recent works [*Vallina et al.*, 2008; *Vallina and Simó*, 2007], enables our model to correctly capture the phase of DMS seasonality in most regions of the ocean (Table 5). Figure 9a shows the Spearman correlation between modeled DMS and interpolated observations from *Kettle and Andreae* [2000]. Both data sets are positively correlated over most regions of the ocean, except for the equatorial regions of the Pacific and the Indian Ocean. Modeled and observed DMS are closely correlated for the Southern Ocean, where correlations lie between 0.4 at ca. 50°S and 0.8–1.0 between 60°S and 70°S. Figure 9 also shows the correlations between model chlorophyll and DMS. In the SEP run, DMS and

Figure 7. Seasonality in (a) DMS, (c) DMSPp, (d) DMSPd, and (e) chlorophyll, as simulated by DMS-PlankTOM (SEP), compared to seasonality of interpolated (b) DMS field from *Kettle and Andreae* [2000] and (f) chlorophyll-a from SeaWiFS. While there is only one maximum in DMS in the high latitudes (bloom regime), there are two DMS maxima in the low latitudes between 40°N and 40°S (stress regime).

chlorophyll are anticorrelated between 20°N and 20°S, in agreement with the data [see *Vallina et al.*, 2006, Figure 1]. Wheras the data shows a larger zone of anticorrelation, our model does not consistently reproduce the decoupling of

DMS and chlorophyll between 20°N(S) and 40°N(S). Between 40°N and 40°S, chlorophyll values are observed to be maximal in spring and minimal in summer, whereas DMS values are maximal in summer (see Figure 7). This

Table 5. Seasonal Correlations Between Modeled and Observed DMS[a]

Ocean Basin	ρ
North Atlantic (40°N–70°N)	0.94
Subtropical Atlantic NH (10°N–40°N)	0.53
Equatorial Atlantic (10°N–10°S)	0.36
Subtropical Atlantic SH (10°S–40°S)	0.64
North Pacific (40°N–70°N)	0.79
Subtropical Pacific NH (10°N–40°N)	0.81
Equatorial Pacific (10°N–10°S)	0.31
Subtropical Pacific SH (10°S–40°S)	0.62
Subtropical Indian Ocean NH (10°N–40°N)	−0.50
Equatorial Indian Ocean (10°N–10°S)	−0.34
Subtropical Indian Ocean SH (10°S–40°S)	0.70
Arctic Ocean (70°N–90°N)	−0.34
Southern Ocean (40°S–60°S)	0.69
Antarctic Ocean (60°S–90°S)	0.94

[a]See *Kettle and Andreae* [2000]. Correlations determined by the Spearman rank correlation coefficient. NH, Northern Hemisphere; SH, Southern Hemisphere.

behavior indicates the existence of two "regimes" in the ocean [*Toole and Siegel*, 2004]: In the bloom-dominated high latitudes, DMS and chlorophyll are closely temporally correlated [*Simó and Dachs*, 2002]. In the stress-forced regime (low latitudes), DMS and chlorophyll dynamics are no longer in phase and DMS is strongly light dependent.

[44] PlankTOM5-SNEP includes a variable DMSPp cell quota, but does not include the DMS exudation term (Table 4). Both global annual and zonal mean DMS are in fairly good agreement with observation-based means from [*Kettle and Andreae*, 2000] (Figure 5). However, PlankTOM5-SNEP does not achieve substantial decoupling of DMS and chlorophyll in the low latitudes (Figures 9c and 9d). While cell quotas were variable by a factor of 4, this was still not enough to produce significant decoupling in the low latitudes. In addition, DMSPp concentrations were very high in this model (global annual mean: 32 nM, versus 12 nM for PlankTOM5-SEP). For this run, DMS and chlorophyll were tightly coupled in most regions of the ocean, except for a small zone of antiphasal behavior in the Pacific.

[45] PlankTOM5-SENP (Figures 9e and 9f) assumes equal cell quotas for the 3 pPFTs, but allows the cell quota to vary with environmental stress (light and nutrient availability) and includes the direct DMS exudation term. There is almost no difference between the correlations for PlankTOM5-SEP and for this model. This finding points either at a reduced importance of an individual, PFT-dependent cell quota when compared to the influence of light for reproducing the summer paradox. Alternatively, the results can be interpreted as an insufficient representation of PFT succession in PlankTOM5 (see section 5). Model-data agreement for the annual means is worse for this run than for PlankTOM-SEP (Table 4).

[46] In PlankTOM5-NSENP (Figures 9g and 9h) all PFTs were set to have identical and constant cell quota, with no possibility for an adaptation of the DMSPp cell quota to environmental stress. Here, the correlation between modeled DMS and DMS from the interpolated Kettle database deteriorates, and modeled DMS and chlorophyll-a are coupled almost everywhere in the ocean.

[47] We use the global mean Spearman correlation coefficient ρ^Φ between modeled and observed DMS seasonality as a means to rank the importance of the individual processes. This number can be used to estimate the relative contribution of regions with positive and negative correlation. For PlankTOM5-SEP, we find that $\rho^\Phi = 0.35$, for PlankTOM5-SNEP $\rho^\Phi = 0.05$, for PlankTOM5-SENP $\rho^\Phi = 0.33$ and for PlankTOM5-NSENP $\rho^\Phi = 0.10$. This means, that in our model, exudation is the most important process to correctly simulate DMS seasonality, as its exclusion leads to the largest deterioration in $\Delta\rho^\Phi = 0.3$. The second most important process is the stress-dependent cell quota. Finally, the inclusion of a PFT-specific minimal cell quota does not significantly deteriorate ρ^Φ.

4.3.3. Simulating DMS Seasonality at BATS

[48] We evaluate the model at the Bermuda Atlantic Time Series Station (BATS, 63.5°W, 32.4°N), where DMSPp, DMSPd and DMS patterns were continuously monitored between 1992 and 1993 [*Dacey et al.*, 1998]. This site is known to display the summer paradox [*Simó and Pedrós-Alió*, 1999; *Toole et al.*, 2003; *Dacey et al.*, 1998] and is therefore a suitable test site for model seasonality.

[49] The comparison of modeled and observed DMS (Figures 10a and 10b) shows that DMS surface concentrations are generally well matched by the model. The model exhibits a surface maximum (4–4.5 nM) in April, which is not present in the observations. Hence, it does not simulate DMS production during the spring bloom accurately. However, there is a smaller, second surface DMS maximum in August (2.5–3 nM), where observed DMS concentrations are around 3.5–4 nM. In the vertical distribution, DMS accumulation is relatively low and observed maximal values of up to 6 nM are not captured in the model (up to 4 nM at depths of 30 m). The observed depth of the summer maximum in DMS is well captured by the model (20–30 m), but the magnitude of the subsurface maximum in DMS is underestimated.

[50] The magnitude of surface DMSPd concentrations of model and data are in reasonable agreement (Figures 10c and 10d), with observed DMSPd being 50–100% higher than modeled DMSPd for the summer months (June–September). Given known problems in the methodology for the estimation of DMSPd concentrations using the purge-and-trap technique [*Kiene and Slezak*, 2006], the observational data could be overestimated and should not be overinterpreted. Modeled surface DMSPd peaks in April/May and then again in August, whereas observed DMSPd is high during May–August, and almost constant throughout the water column.

[51] DMSPp is overestimated in the model, in particular during the spring months, where model concentrations rise up to 30 nM (Figures 10e and 10f). Observed DMSPp is only about 12 nM at the surface and maximum DMSPp is reached at a depth of 50 m (16 nM). While the model accumulates DMSPp (10–15 nM) at 70–90 m depth during the summer and autumn months, observed DMSPp is maximal only in May and June and rapidly drops below 10 nM for the entire water column.

[52] Total chlorophyll is compared in Figures 10g and 10h. The model overpredicts chlorophyll during the spring bloom, and it underpredicts the deep chlorophyll maximum during the summer months at 80 m depth. In particular, the
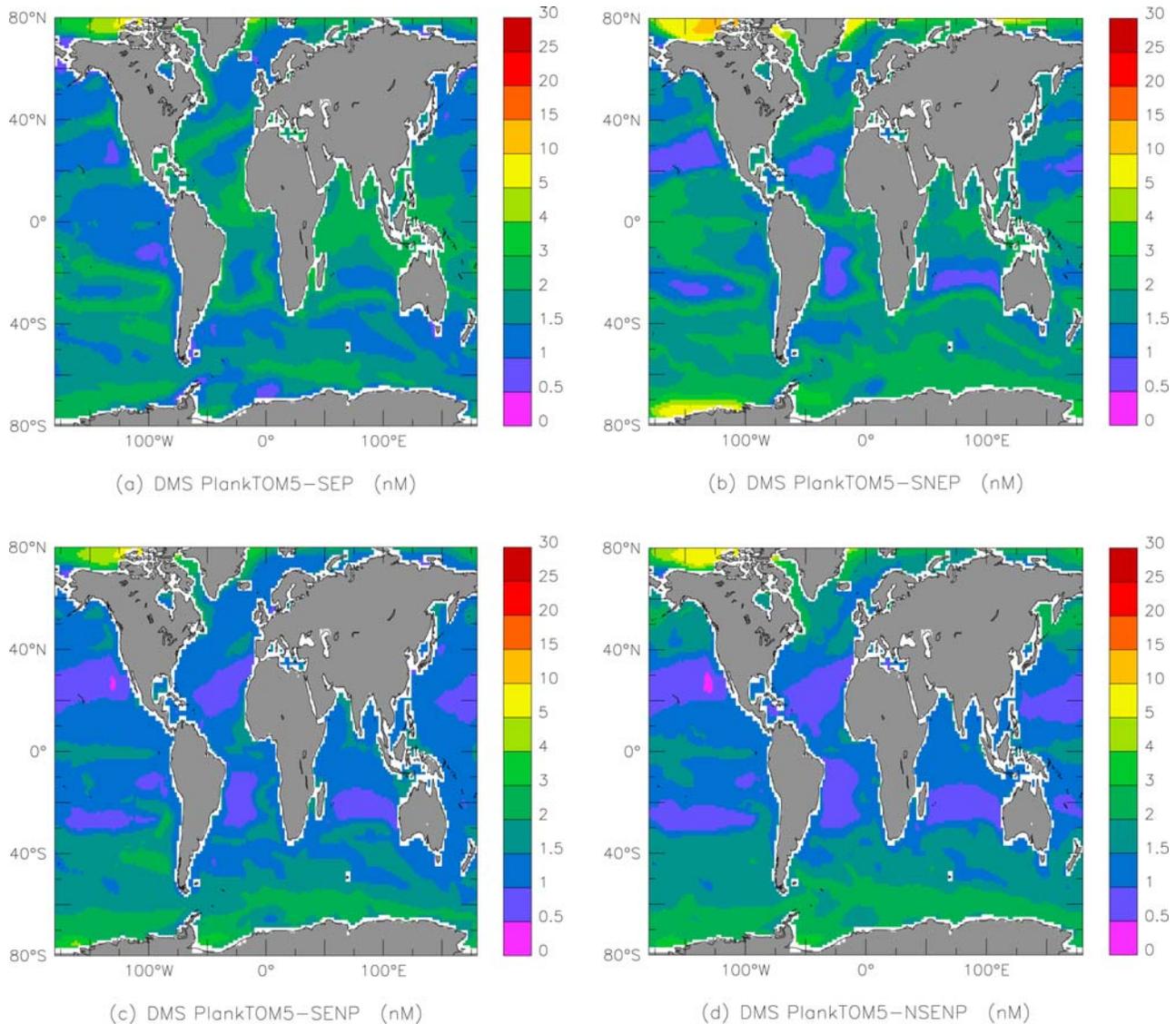
Figure 8. Annual mean DMS fields (nM) for the four test runs: (a) standard run, PlankTOM5-SEP; (b) PlankTOM5-SNEP; (c) PlankTOM5-SENP; and (d) PlankTOM5-NSENP. PlankTOM-SEP (Figure 8a) has been tuned to best fit DMS seasonality. PlankTOM-SNEP (Figure 8b) has been tuned to best fit annual mean sea surface DMS from *Kettle and Andreae* [2000].

modeled high surface chlorophyll in April is not observed. A comparison of Figures 10e and 10f with Figures 10g and 10h shows, that DMSPp and chlorophyll are intrinsically coupled in the model but less so in the observations. Decoupling between chlorophyll and the modeled sulphur compounds is only achieved in DMSPd and to a lesser extent in DMS. This points at the importance of a variable DMSPp cell quota at BATS, as highlighted by *Le Clainche et al.* [2004]. In PlankTOM5, we could not achieve decoupling of DMS and chlorophyll-a through a variable cell quota only.

5. Discussion

5.1. DMS Concentrations and Global DMS Seasonality

[53] Our model simulates the concentrations of DMS, DMSPd and DMSPp within the global ocean biogeochem-istry model PlankTOM5, which includes 3 pPFTs and 2 zPFTs. In contrast to other models [e.g., *Six and Maier-Reimer*, 2006], this model was tuned to better represent DMS seasonality for the global ocean, while still giving realistic global and zonal mean concentrations. In the model, DMS seasonality in the temperate and high latitudes is driven by phytoplankton biomass, where DMS and chloro-phyll are coupled. The inclusion of an explicit light-dependent term [*Sunda et al.*, 2002; *Vallina et al.*, 2008] leads to a decoupling of DMS and chlorophyll in the tropics and to a better representation of global DMS seasonality. Hence, the model shows two distinct regimes, a "bloom-forced regime" and a "stress-forced regime," as postulated by *Toole and Siegel* [2004].

[54] A classical parameter sensitivity test (section 4.2.3) showed that simulated global annual mean DMS con-centrations are particularly sensitive to the internal DMSP
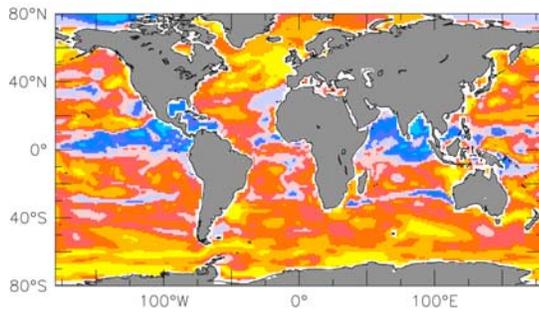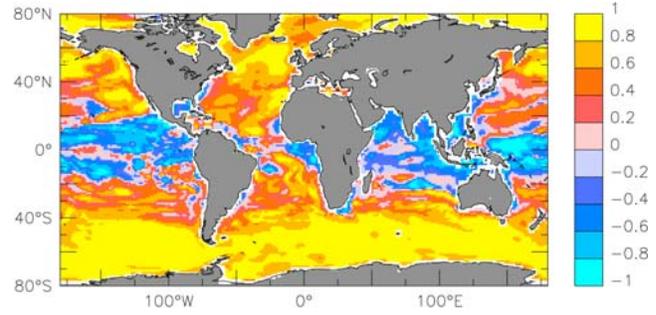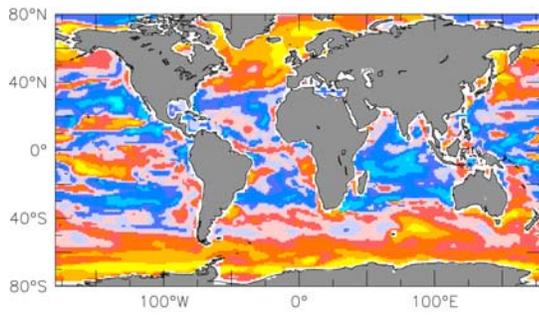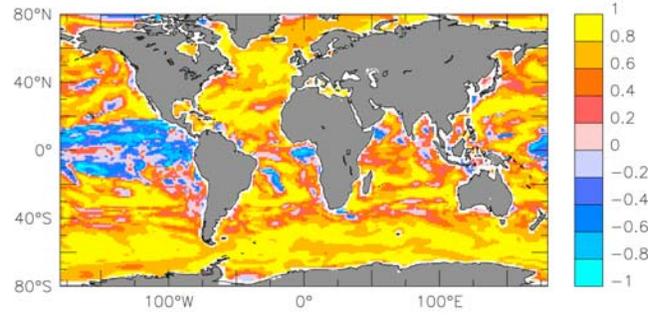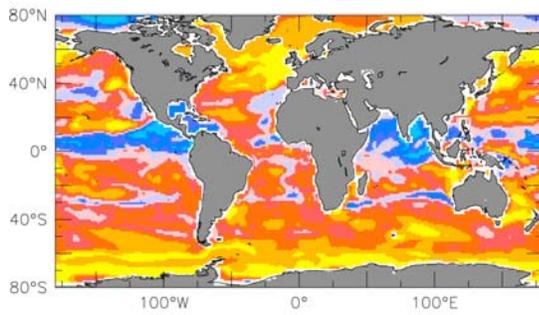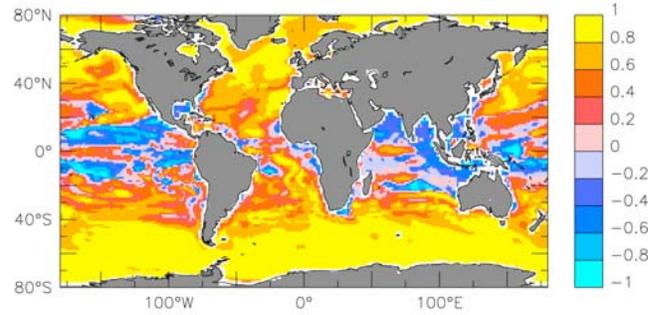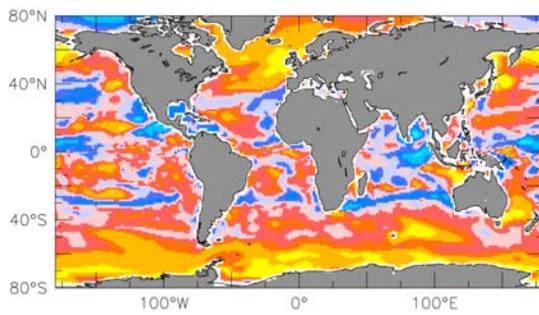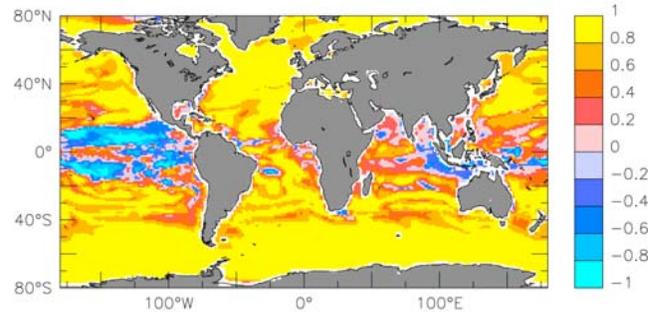
Figure 9. (left) Correlations between DMS from *Kettle* [2000] and DMS from the four test runs using DMS-PlankTOM5. (right) Correlations between DMS in PlankTOM5 and chlorophyll-a for the four different test runs using DMS-PlankTOM5. (a and b) PlankTOM5-SEP, (c and d) PlankTOM5-SNEP, (e and f) PlankTOM5-SENP, and (g and h) PlankTOM5-NSENP. Observed and modeled DMS are more strongly positively correlated in the low latitudes in Figures 9a and 9e. Accordingly, the observed decoupling between DMS and chlorophyll between 40°N and 40°S (summer paradox [*Toole et al.*, 2003]) is captured better by the model in Figures 9b and 9f than in Figures 9d and 9h.
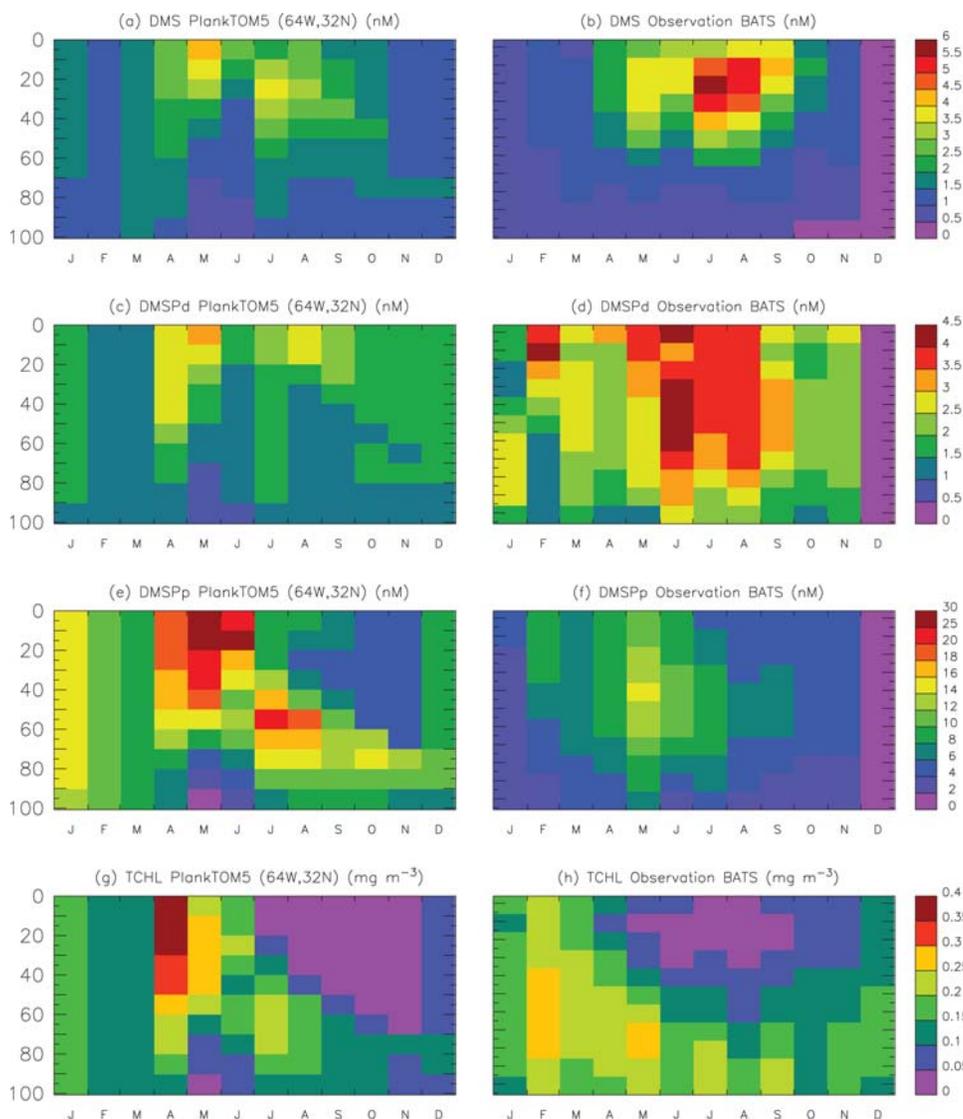
Figure 10. Comparison of (left) modeled (from PlankTOM5-SEP) and (right) observed (a and b) DMS, (c and d) DMSPd, (e and f) DMSPp, and (g and h) chlorophyll from the Bermuda Atlantic Time Series Stations (BATS) at depths of 0–100 m. Model values correspond to those at coordinates 32°N, 64°W and are averaged over 1° × 1°.

cell quota and the DMS exudation rates. Furthermore, global mean DMS concentrations respond strongly to bacterial parameters such as the bacterial temperature dependence. Other models confirm the importance of these key parameters: *Six and Maier-Reimer* [2006] find that bacterial activity is crucial for DMS concentration patterns, and the importance of bacterial parameters has also been confirmed in 1-D studies [*Vallina et al.*, 2008]. Several other models agree that cell quota are a key parameter for model results [*Lefèvre et al.*, 2002; *Le Clainche et al.*, 2004; *Vallina et al.*, 2008].

[55] Model simulations with a variable DMS cell quota but no external light driven terms led to the best fit regarding zonal annual mean concentrations, but in the low latitudes DMS seasonality was out of phase with observations. This effect may result from the data treatment applied by *Kettle and Andreae* [2000]: The authors used information on bio-

geochemical provinces (and hence chlorophyll concentration levels) to generate interpolated DMS fields. This approach will influence observation-based zonal means and couple them more strongly to chlorophyll-a. Alternatively, zonal mean DMS may be intrinsically linked to observed chlorophyll levels, so that total biomass controls the baseline level for mean DMS concentrations.

[56] PlankTOM5 is one of the first global prognostic models that is capable of simulating global DMS seasonality correctly. Some other global prognostic DMS models cannot simulate the summer paradox [*Six and Maier-Reimer*, 2006; *Kloster et al.*, 2006; *Aumont and Bopp*, 2006]. The model described by *Chu et al.* [2003] is capable of a certain decoupling, but it uses location-dependent DMS generation formulae. We now combine several stressors, and use only one set of equations for the entire ocean.

5.2. DMS and the Summer Paradox

[57] We tested the relative importance of phytoplankton succession, changes in the DMSP cell quota and the direct release of DMS from light-stressed phytoplankton cells for DMS seasonality in the tropics. We find that exudation is the most important process for DMS seasonality in the low latitudes, and that a variable cell quota is more important than a PFT-specific cell quota. In PlankTOM5, light is the dominant driver for DMS seasonality in the low latitudes, and phytoplankton biomass drives DMS seasonality in the mid- and high latitudes.

[58] Given that PlankTOM5 currently only comprises of 3 pPFTs, it is premature to conclude that ecosystem composition is of minor importance for DMS seasonality. Especially at low latitudes, the ecosystem of PlankTOM5 is mostly dominated by the group of the mixed phytoplankton, while diatoms occur predominantly at high latitudes. Calcifiers dominate in defined zonal bands in the NH. Hence, the modeled ocean is dominated by one or two types of phytoplankton over large regions of the globe. This restricts the potential influence of species succession and ecosystem composition on DMS patterns.

[59] Local 1-D models achieved decoupling either through a light-dependent DMSP cell quota [Lefèvre et al., 2002; Le Clainche et al., 2004] or through the introduction of direct DMS generation terms from algal cells [Vallina et al., 2008; Toole et al., 2008]. In our global model, a change in cell quota alone as a response to light stress in conjunction with species succession was not sufficient to reach a satisfactory decoupling in the low latitudes. In particular, the model only produces a summer paradox at BATS after the introduction of an exudation term.

[60] Whether DMS dynamics in the low latitudes are driven by exudation, i.e., the active or passive transport of DMS across the cell membrane, or by another process with a similar signature, e.g., the phytoplanktonic cleavage of DMSPd by (extracellular) DMSP lyase [Niki et al., 2000] or bacterial and bacteria-mediated process, is not yet certain. At present, the experimental evidence for exudation is scarce [see, e.g., Stefels et al., 2007]. The importance of bacterial processes for DMS seasonality has not been evaluated in this study, due to the coarseness of our representation of bacterial dynamics. Several bacterial processes have been found to be light sensitive, and may contribute to the summer paradox: Bacterial consumption of DMS is inhibited at high light intensities [Slezak et al., 2001], the microbial yield of DMS from DMSP can vary with bacterial sulphur demand, which may be dependant on UV stress [Simó and Pedrós-Alió, 1999; Kiene et al., 2000]. These processes may explain parts of the summer paradox.

5.3. Model Results at the BATS Site

[61] It is important to note that our model was not developed to fit the time series at the Bermuda Atlantic Time Series Station. We constructed the model to better reproduce global seasonality of DMS concentrations at all latitudes, and DMS(P) values at BATS were only evaluated a posteriori after model development was finalized. A global 3-D model with its coarse grid is not optimally suited to accurately resolve the dynamics at one specific location. However, the time series data allows to test whether

PlankTOM5 can resolve the depth structure of the seasonal DMS cycle. As can be seen in Figure 9, the Sargasso Sea is one of the regions where we do not yet achieve a complete decoupling between DMS and chlorophyll values. Given that a 1° × 1° mean is compared to point measurements in a region where a strong influence of small scale physics (eddies) has been shown to play an important role [Le Clainche et al., 2004; Bailey et al., 2008], the agreement between model and measurement is reasonable.

[62] Observations at BATS point at a phase lag between surface DMSPp and surface chlorophyll, which the model does not reproduce well, despite the fact that we model variable DMSP cell quotas. Variable DMSP cell quotas could enable decoupling, if reduced sinks allowed a stronger accumulation of DMS, and if ecosystem composition and succession were well represented. We achieve a certain degree of decoupling between DMS and chlorophyll through the introduction of an exudation term, which supports findings by Vallina and Simó [2007] and Vallina et al. [2008]. However, Le Clainche et al. [2004] reach a best model data fit for BATS through a variable DMSP cell quota without direct DMS exudation. Hence, other processes may be responsible for parts of the observed patterns.

[63] The simulation of the dynamics in a real marine ecosystem is challenging for any model containing only a limited number of PFTs. At BATS, phytoplanktonic community composition has been found to be dominated by cyanobacteria [Andersen et al., 1996; Goericke, 1998; Steinberg et al., 2001]. In the model, however, the spring bloom at BATS is dominated by diatoms and coccolithophores, whereas the dominant observed groups at BATS almost exclusively belong to our mixed PFT. In contrast to nanophytoplankton, cyanobacteria tend to be poor DMS producers. While the overestimation of DMSPp during the spring bloom is due to the overestimation in phytoplanktonic biomass, the underestimation of DMS during the summer is likely due to a suboptimal modelization of DMSPd and DMS sinks and the microbial loop.

6. Summary and Conclusion

[64] We have built a global DMS model that takes into account DMS production and degradation mechanisms dependent on external factors such as environmental temperature and insolation. The model reproduces global seasonality of DMS and partly captures the summer paradox observed between 40°N and 40°S. Our model results suggest that DMS seasonality in the low latitudes is driven by light, and by phytoplankton biomass in the high latitudes. Zonal and global mean DMS appear to be sensitive to ecosystem composition and phytoplankton biomass. In our model, the improvement of DMS seasonality leads to the deterioration of the zonal mean concentrations, and it is not yet clear whether this is an artifact of the data treatment, or whether this finding is an indication that exudation, or a process with a similar signature, acts in concert with other processes, leading to a superposition of zonal and seasonal dynamics.

[65] Here, we focus on the relative importance of ecosystem composition and dynamics and light stress for the seasonality of DMS at different latitudes, and chose exudation as one possible process by which algal DMS

production can be made light dependent. Several other mechanisms to explain the summer paradox have been proposed, such as a species succession from low to high DMS-producing phytoplankton, the inhibition of bacterial DMS degradation under UV stress, or a variation in bacterial sulphur demand. One major caveat of PlankTOM5 is the coarse parameterization of bacterial dynamics. More comprehensive studies are needed that study the role of the microbial loop for the summer paradox. While our current study confirms the importance of light, it is still possible that other, unmodeled processes with a similar signature to our exudation pathway account for (parts of) the summer paradox. Future modeling studies should use DGOMs with a complexity higher than the one of PlankTOM5 (must include bacteria) and should address all possible processes that can lead to the decoupling of DMS and chlorophyll in the low latitudes. In particular, it is necessary to quantify the relative importance of bacteria-mediated process and phytoplanktonic processes. Furthermore, it is still difficult to simulate biogeographic patterns with only 3 pPFTs. DMS dynamics and concentration patterns are highly sensitive to many ecosystem processes across trophic levels. DMS can serve as a test compound for the next generation of DGOMs, if key PFTs, such as *Phaeocystis* are included. While we do not find pPFT distribution to be highly important for DMS seasonality in this work, other authors have been able to reproduce DMS seasonality at BATS without resorting to exudation [*Le Clainche et al.*, 2004]. Hence, it is premature to conclude that ecosystem composition is of minor importance for DMS concentration patterns.

References

Allen, J. I., P. J. Somerfield, and F. J. Gilbert (2007), Quantifying uncertainty in high-resolution coupled hydrodynamic-ecosystem models, *J. Mar. Syst.*, 64(1–4), 3–14.

Alvain, S., C. Moulin, Y. Dandonneau, and F. M. Bréon (2005), Remote sensing of phytoplankton groups in case I waters from global SeaWiFS imagery, *Deep Sea Res. Part I*, 52(11), 1989–2004.

Alvain, S., C. Moulin, Y. Dandonneau, H. Loisel, and F. M. Bréon (2006), A species-dependent bio-optical model of case I waters for global ocean color processing, *Deep Sea Res. Part I*, 53(5),917–925.

Alvain, S., C. Moulin, Y. Dandonneau, and H. Loisel (2008), Seasonal distribution and succession of dominant phytoplankton groups in the global ocean: A satellite view, *Global Biogeochem. Cycles*, 22, GB3001, doi:10.1029/2007GB003154.

Andersen, R. A., R. R. Bidigare, M. D. Keller, and M. Latasa (1996), A comparison of HPLC pigment signatures and electron microscopic observations for oligotrophic waters of the North Atlantic and Pacific oceans, *Deep Sea Res. Part II*, 43(2–3), 517–537.

Archer, S. D., F. J. Gilbert, P. D. Nightingale, M. V. Zubkov, A. H. Taylor, G. C. Smith, and P. H. Burkill (2002), Transformation of dimethylsulphoniopropionate to dimethyl sulphide during summer in the North Sea with an examination of key processes via a modelling approach, *Deep Sea Res. Part II*, 49, 3067–3101.

Aumont, O., and L. Bopp (2006), Globalizing results from ocean in situ iron fertilization studies, *Global Biogeochem. Cycles*, 20, GB2017, doi:10.1029/2005GB002591.

Bailey, K. E., D. A. Toole, B. Blomquist, R. G. Najjar, B. Huebert, D. J. Kieber, R. P. Kiene, R. Matrai, G. R. Westby, and D. A. del Valle (2008), Diemthylsulfide production in Sargasso Sea eddies, *Deep Sea Res. Part II*, 55(10–13), 1491–1504.

Behrenfeld, M. J., and P. G. Falkowski (1997), Photosynthetic rates derived from satellite-based chlorophyll concentration, *Limnol. Oceanogr.*, 42(1), 1–20.

Bell, T. G., G. Malin, C. M. McKee, and P. S. Liss (2006), A comparison of dimethylsulphide (DMS) data from the Atlantic Meridional Transect (AMT) programme with proposes algorithms for global surface DMS concentrations, *Deep Sea Res. Part II*, 53(14–16), 1720–1735, doi:10.1016/j.dsr2.2006.05.013.

Belviso, S., L. Bopp, C. Moulin, J. C. Orr, T. R. Anderson, O. Aumont, S. Chu, S. Elliott, M. E. Maltrud, and R. Simó (2004), Comparison of global climatological maps of sea surface dimethyl sulfide, *Global Biogeochem. Cycles*, 18, GB3013, doi:10.1029/2003GB002193.

Blackman, R. B., and J. W. Tukey (1959), Particular pairs of windows, in *The Mesurement of Power Spectra From the Point of View of Communications Engineering*, pp. 98–99, Dover, New York.

Bopp, L., O. Aumont, S. Belviso, and S. Blain (2008), Modelling the effect of iron fertilization on dimethylsulphide emissions in the Southern Ocean, *Deep Sea Res. Part II*, 55(5–7), 901–912, doi:10.1016/j.dsr2.2007.12.002.

Brimblecombe, P., and D. Shooter (1986), Photooxidation of dimethylsulfide in aqueous-solution, *Mar. Chem.*, 19(4), 343–353.

Brugger, A., D. Slezak, I. Obernosterer, and G. J. Herndl (1998), Photolysis of dimethylsulfide in the northern Adriatic Sea: Dependence on substrate concentration, irradiance and doc concentration, *Mar. Chem.*, 59(3–4), 321–331.

Buitenhuis, E., P. van der Wal, and H. de Baar (2001), Blooms of *Emiliania huxleyi* are sinks of atmospheric carbon dioxide: A field and mesocosm study derived simulation, *Global Biogeochem. Cycles*, 15, 577–588, doi:10.1029/2000GB001292.

Buitenhuis, E., C. Le Quéré, O. Aumont, G. Beaugrand, A. Bunker, A. Hirst, T. Ikeda, T. O'Brien, S. Piontkovski, and D. Straile (2006), Biogeochemical fluxes through mesozooplankton, *Global Biogeochem. Cycles*, 20, GB2003, doi:10.1029/2005GB002511.

Calbet, A. (2001), Mesozooplankton grazing effect on primary production: A global comparative analysis in marine ecosystems, *Limnol. Oceanogr.*, 46, 1824–1830.

Calbet, A., and M. R. Landry (2004), Phytoplankton growth, microzooplankton grazing, and carbon cycling in marine systems, *Limnol. Oceanogr.*, 49, 51–57.

Charlson, R. J., J. E. Lovelock, M. O. Andreae, and S. G. Warren (1987), Oceanic phytoplankton, atmospheric sulfur, cloud albedo and climate, *Nature*, 326(6114), 655–661.

Chu, S., S. Elliott, and M. E. Maltrud (2003), Global eddy permitting simulations of surface ocean nitrogen, iron, sulphur cycling, *Chemosphere*, 50, 223–235.

Cropp, R. A., J. Norbury, A. J. Gabric, and R. D. Braddock (2004), Modelling dimethylsulphide production in the upper ocean, *Global Biogeochem. Cycles*, 18, GB3005, doi:10.1029/2003GB002126.

Curson, A. R. J., R. Rogers, J. D. Todd, C. A. Brearley, and A. W. B. Johnston (2008), Molecular genetic analysis of a dimethylsulfoniopropionate lyase that liberates the climate-changing gas demethylsulfide in several marine α-proteobacteria and *Rhodobacter sphaeroides*, *Environm. Microbiol.*, 10(3), 757–767, doi:10.1111/j.1462-2920.2007.01499.x.

Dacey, J. W. H., F. A. Howse, A. F. Michaels, and S. G. Wakeham (1998), Temporal variability of dimethylsulphoniopropionate and dimethylsulphide in the Sargasso Sea, *Deep Sea Res. Part I*, 45, 2085–2104.

da Cunha, L., E. T. Buitenhuis, C. Le Quéré, X. Giraud, and W. Ludwig (2007), Potential impact of changes in river nutrient supply on global ocean biogeochemistry, *Global Biogeochem. Cycles*, 21, GB4007, doi:10.1029/2006GB002718.

Dickson, D. M. J., and G. O. Kirst (1986), The role of beta-dimethylsulphoniopropionate, glycine betaine and homarine in the osmoacclimation of Platymonas subcordiformis, *Planta*, 167(4), 536–543.

Dickson, D. M. J., and G. O. Kirst (1987a), Osmotic adjustment in marine eukaryotic algae: The role of inorganic ions, quaternary ammonium, tertiary sulfonium and carbohydrate solutes. Part 1. Diatoms and a rhodophyte, *New Phytol.*, 106(4), 645–655.

Dickson, D. M. J., and G. O. Kirst (1987b), Osmotic adjustment in marine eukaryotic algae: The role of inorganic ions, quaternary ammonium, tertiary sulfonium and carbohydrate solutes. Part 2. Prasinophytes and haptophytes, *New Phytol.*, 106(4), 657–666.

Fichefet, T., and M. A. M. Maqueda (1999), Modelling the influence of snow accumulation and snow-ice formation on the seasonal cycle of the Antarctic sea-ice cover, *Clim. Dyn.*, *15*(4), 251–268.

Gasper, P. Y., Y. Gregoris, and J. M. Lefèvre (1990), A simple kinetic kinetic energy model for simulations on the ocean vertical mixing: Tests at station Papa and longer upper ocean study site, *J. Geophys. Res.*, *95*, 16,179–16,193.

Goericke, R. (1998), Response of phytoplankton community structure and taxon-specific growth rates to seasonally varying physical forcing in the Sargasso Sea off Bermuda, *Limnol. Oceanogr.*, *43*(5), 921–935.

Karsten, U., C. Wiencke, and G. O. Kirst (1992), Dimethylsulphoniopropionate (DMSP) accumulation in green macroalgae from polar to temperate regions - interactive effects of light versus salinity and light versus temperature, *Polar Biol.*, *12*(6–7), 603–607.

Karsten, U., K. Kuck, C. Vogt, and G. O. Kirst (1996), Dimethylsulfoniopropionate production in phototrophic organisms and its physiological function as a cryoprotectant, in *Biological and Environmental Chemistry of DMSP and Related Sulfonium Compounds*, edited by Ronald P. Kiene et al., pp. 143–153, Plenum, New York.

Keller, M. D., W. K. Bellows, and R. R. L. Guillard (1989), Dimethyl sulfide production in marine phytoplankton, *ACS Symp. Ser.*, *393*, 167–182.

Kettle, A. J., and M. O. Andreae (2000), Flux of dimethylsulfide from the oceans: A comparison of updated data seas and flux models, *J. Geophys. Res.*, *105*(D22), 26,793–26,808.

Kettle, A. J., et al. (1999), A global database of sea surface dimethyl sulfide (DMS) measurements and a procedure to predict sea surface dms as a function of latitude, longitude, and month, *Global Biogeochem. Cycles*, *13*(2), 399–444.

Key, R. M., A. Kozyr, C. L. Sabine, K. Lee, R. Wanninkhof, J. L. Bullister, R. A. Feely, F. J. Millero, C. Mordy, and T.-H. Peng (2004), A global ocean carbon climatology: Results from Global Data Analysis Project (GLODAP), *Global Biogeochem. Cycles*, *18*, GB4031, doi:10.1029/2004GB002247.

Kieber, D. J., J. F. Jiao, R. P. Kiene, and T. S. Bates (1996), Impact of dimethylsulfide photochemistry on methyl sulfur cycling in the equatorial Pacific Ocean, *J. Geophys. Res.*, *101*(C2), 3715–3722.

Kiene, R. P., and D. Slezak (2006), Low dissolved DMSP concentrations in seawater revealed by small-volume gravity filtration and dialysis sampling, *Limnol. Oceanogr.*, *4*, 80–95.

Kiene, R. P., L. J. Linn, and J. A. Bruton (2000), New and important roles for DMSP in marine microbial communities, *J. Sea Res.*, *43*(3–4), 209–224.

Kloster, S., J. Feichter, E. M. Reimer, K. D. Six, P. Stier, and P. Wetzel (2006), DMS cycle in the marine ocean-atmosphere system: A global model study, *Biogeosciences*, *3*(1), 29–51.

Le Clainche, Y., M. Levasseur, A. Vézina, J. W. H. Dacey, and F. J. Saucier (2004), Behviour of the ocean DMS(P) pools in the Sargasso Sea viewed in a coupled physical-biogeochemical ocean model, *Can. J. Fish. Aquat. Sci.*, *61*(5), 788–803.

Lefèvre, M., A. Vézina, M. Levasseur, and J. W. H. Dacey (2002), A model of dimethylsulfide dynamics for the subtropical North Atlantic, *Deep Sea Res. Part I*, *49*(12), 2221–2239.

Le Quéré, C., et al. (2005), Ecosystem dynamics based on plankton functional types for global ocean biogeochemistry models, *Global Change Biol.*, *11*(11), 2016–2040.

Le Quéré, C., et al. (2007), Saturation of the Southern Ocean sink due to recent climate change, *Science*, *316*(5832), 1735–1738, doi:10.1126/science.1136188.

Liss, P. S., and P. G. Slater (1974), Flux of gases across air-sea interface, *Nature*, *247*(5438), 181–184.

Madec, G., P. Delecluse, M. Imbard, and C. Lévy (1998), OPA 8.1 ocean general circulation model reference manual, *Note Pole Model. 11*, Inst. Pierre-Simon Laplace, Paris.

Malin, G., W. H. Wilson, G. Bratbak, P. S. Liss, and N. H. Mann (1998), Elevated production of dimethylsulfide resulting from viral infection of cultures of *phaeocystis pouchetii*, *Limnol. Oceanogr.*, *43*(6), 1389–1393.

Maréchal, D. (2004), A soil-based approach to rainfall-runoff modelling in ungauged catchments for England and Wales, Ph.D. thesis, Cranfield Univ., Cranfield, U. K.

Nguyen, B. C., S. Belviso, N. Mihalopoulos, J. Gostan, and P. Nival (1988), Dimethyl sulfide production during natural phytoplanktonic blooms, *Mar. Chem.*, *24*(2), 133–141.

Niki, T., M. Kunugi, and A. Otsuki (2000), DMSP-lyase activity on five marine phytoplankton species: Its potential importance in DMS production, *Mar. Biol.*, *136*(5), 759–764.

Saltzman, E. S., D. B. King, K. Holmen, and C. Leck (1993), Experimental-determination of the diffusion-coefficient of dimethylsulfide in water, *J. Geophys. Res.*, *98*(C9), 16,481–16,486.

Scarratt, M., G. Cantin, M. Levasseur, and S. Michaud (2000), Particle size-fractionated kinetics of DMS production: Where does DMSP cleavage occur at the microscale?, *J. Sea Res.*, *43*(3–4), 245–252.

Schlitzer, R. (2004), Export production in the equatorial and North Pacific derived from dissolved oxygen, nutrient and carbon data, *J. Oceanogr.*, *60*(1), 53–62.

Simó, R., and J. Dachs (2002), Global ocean emission of dimethylsulfide predicted from biogeophysical data, *Global Biogeochem. Cycles*, *16*(4), 1018, doi:10.1029/2001GB001829.

Simó, R., and C. Pedrós-Alió (1999), Short-term variability in the open ocean cycle of dimethylsulfide, *Global Biogeochem. Cycles*, *13*(4), 1173–1181.

Six, K. D., and E. Maier-Reimer (2006), What controls the oceanic dimethylsulfide (DMS) cycle? A modeling approach, *Global Biogeochem. Cycles*, *20*, GB4011, doi:10.1029/2005GB002674.

Slezak, D., A. Brugger, and G. J. Herndl (2001), Impact of solar radiation on the biological removal of dimethylsulfoniopropionate and dimethylsulfide in marine surface waters, *Aquat. Microbiol. Ecol.*, *25*(1), 87–97.

Stefels, J., M. Steinke, S. Turner, G. Malin, and S. Belviso (2007), Environmental constraints on the production and removal of the climatically active gas dimethylsulphide (DMS) and implications for ecosystem modelling, *Biogeochemistry*, *83*(1–3), 245–275.

Steinberg, D. K., C. A. Carlson, N. R. Bates, R. J. Johnson, A. F. Michaels, and A. H. Knap (2001), Overview of the US JGOFS Bermuda Atlantic Time-series Study (BATS): A decade-scale look at ocean biology and biogeochemistry, *Deep Sea Res. Part II*, *48*(8–9), 1405–1447.

Sunda, W., D. J. Kieber, R. P. Kiene, and S. Huntsman (2002), An antioxidant function for DMSP and DMS in marine algae, *Nature*, *418*(6895), 317–320.

Tegen, I., and I. Fung (1995), Contribution to the atmospheric mineral aerosol load from land-surface modification, *J. Geophys. Res.*, *100*(D9), 18,707–18,726.

Timmermann, R., H. Goosse, G. Madec, T. Fichefet, C. Ethe, and V. Duliere (2005), On the representation of high latitude processes in the ORCA-LIM global coupled sea ice-ocean model, *Ocean Modell.*, *8*(1–2), 175–201.

Todd, J. D., R. Rogers, Y. G. Li, M. Wexler, P. L. Bond, L. Sun, A. R. J. Curson, G. Malin, M. Steinke, and A. W. B. Johnston (2007), Structural and regulatory genes required to make the gas dimethyl sulfide in bacteria, *Science*, *315*(5812), 666–669.

Todd, J. D., A. R. J. Curson, C. L. Dupont, P. Nicholson, and A. W. B. Johnston (2009), The *dddP* gene, encoding a novel enzyme that converts dimethylsulfoniopropionate into dimethyl sulfide, is widespread in ocean metagenomes and marine bacteria and also occurs in some Ascomycete fungi, *Environ. Microbiol.*, *11*(6), 1376–1385, doi:10.1111/j.1462-2920.2009.01864.x.

Toole, D. A., and D. A. Siegel (2004), Light-driven cycling of dimethylsulfide (DMS) in the Sargasso Sea: Closing the loop, *Geophys. Res. Lett.*, *31*, L09308, doi:10.1029/2004GL019581.

Toole, D. A., D. J. Kieber, R. P. Kiene, D. A. Siegel, and N. B. Nelson (2003), Photolysis and the dimethylsulfide (DMS) summer paradox in the Sargasso Sea, *Limnol. Oceanogr.*, *48*(3), 1088–1100.

Toole, D. A., D. A. Siegel, and S. C. Doney (2008), A light-driven, one-dimensional dimethylsulfide cycling model for the Sargasso Sea, *J. Geophys. Res.*, *113*, G02009, doi:10.1029/2007JG000426.

Uitz, J., H. Claustre, A. Morel, and S. B. Hooker (2006), Vertical distribution of phytoplankton communities in open ocean: An assessment based on surface chlorophyll, *J. Geophys. Res.*, *111*, C08005, doi:10.1029/2005JC003207.

Vairavamurthy, A., M. O. Andreae, and R. L. Iverson (1985), Biosynthesis of dimethylsulfide and dimethylpropiothetin by *Hymenomonas carterae* in relation to sulfur source and salinity variations, *Limnol. Oceanogr.*, *30*(1), 59–70.

Vallina, S. M., and R. Simó (2007), Strong relationship between DMS and the solar radiation dose over the global surface ocean, *Science*, *315*, 506–508.

Vallina, S. M., R. Simó, and S. Gasso (2006), What controls CCN seasonality in the Southern Ocean? A statistical analysis based on satellite-derived chlorophyll and CCN and model-estimated OH radical and rainfall, *Global Biogeochem. Cycles*, *20*, GB1014, doi:10.1029/2005GB002597.

Vallina, S. M., R. Simó, S. Gasso, C. De Boyer-Montegut, E. del Rio, E. Jurado, and J. Dachs (2007), Analysis of a potential "solar radiation dose-dimethylsulfide-cloud condensation nuclei" link from globally mapped seasonal correlations, *Global Biogeochem. Cycles*, *21*, GB2004, doi:10.1029/2006GB002787.

Vallina, S. M., R. Simó, T. R. Anderson, A. Gabric, R. Cropp, and J. M. Pacheco (2008), A dynamic model of oceanic sulfur (DMOS) applied to the Sargasso Sea: Simulating the dimethylsulfide (DMS) summer paradox, *J. Geophys. Res.*, 113, G01009, doi:10.1029/2007JG000415.

Vantrepotte, V., and F. Mélin (2006), UV penetration in the water column, *Rep. EUR 22217 EN*, 67 pp., Dir. Gen. Joint Res. Cent., Inst. for Environ. and Sustainability, Luxembourg.

Vila-Costa, M., D. A. del Valle, J. M. Gonzalez, D. Slezak, R. P. Kiene, O. Sanchez, and R. Simó (2006), Phylogenetic identification and metabolism of marine dimethylsulfide-consuming bacteria, *Environ. Microbiol.*, 8(12), 2189–2200.

von Glasow, R., and P. J. Crutzen (2004), Model study of multiphase DMS oxidation with a focus on halogens, *Atmos. Chem. Phys.*, 4, 589–608.

Wanninkhof, R. (1992), Relationship between wind-speed and gas-exchange over the ocean, *J. Geophys. Res.*, 97(C5), 7373–7382.

Wolfe, G. V., and M. Steinke (1996), Grazing-activated production of dimethyl sulfide (DMS) by two clones of *Emiliania huxleyi*, *Limnol. Oceanogr.*, 41(6), 1151–1160.

Zemmelink, H. J., J. W. H. Dacey, and E. J. Hintsa (2004a), Direct measurements of biogenic dimethylsulphide fluxes from the oceans: S synthesis, *Can. J. Fish. Aquat. Sci.*, 61(5), 836–844.

Zemmelink, H. J., J. W. H. Dacey, E. J. Hintsa, W. R. McGillis, W. W. C. Gieskes, W. Klaassen, H. W. de Groot, and H. J. W. de Baar (2004b), Fluxes and gas transfer rates of the biogenic trace gas DMS derived from atmospheric gradients, *J. Geophys. Res.*, 109, C08S10, doi:10.1029/2003JC001795.

Zubkov, M. V., B. M. Fuchs, S. D. Archer, R. P. Kiene, R. Amann, and P. H. Burkill (2001), Linking the composition of bacterioplankton to rapid turnover of dissolved dimethylsulphoniopropionate in an algal bloom in the North Sea, *Environ. Microbiol.*, 3(5), 304–311.

L. Bopp, Laboratoire des Sciences du Climate et de l'Environnement, IPSL, CEA Saclay, CNRS, Orme des Merisiers, Bât 709, F-91191 Gif-sur-Yvette, France.

E. T. Buitenhuis, C. Le Quéré, S. M. Vallina, and M. Vogt, School of Environmental Sciences, University of East Anglia, Norwich NR4 7TJ, UK. (m.vogt@uea.ac.uk)